

Microscopic Dynamics of thin hard rods

Matthias Otto, Timo Aspelmeier and Annette Zippelius

Institut für Theoretische Physik, Friedrich-Hund-Platz 1, D-37077 Göttingen, Germany

Abstract

We analyze the microscopic dynamics and transport properties of a gas of thin hard rods. Based on the collision rules for hard needles we derive a hydrodynamic equation that determines the coupled translational and rotational dynamics of a tagged thin rod in an ensemble of identical rods. Specifically, based on a Pseudo-Liouville operator for binary collisions between rods, the Mori-Zwanzig projection formalism is used to derive a continued fraction representation for the correlation function of the tagged particle's density, specifying its position and orientation. Truncation of the continued fraction gives rise to a generalised Enskog equation, which can be compared to the phenomenological Perrin equation for anisotropic diffusion. Only for sufficiently large density do we observe anisotropic diffusion, as indicated by an anisotropic mean square displacement, growing linearly with time. For lower densities, the Perrin equation is shown to be an insufficient hydrodynamic description for hard needles interacting via binary collisions. We compare our results to simulations and find excellent quantitative agreement for low densities and qualitative agreement for higher densities.

I. INTRODUCTION

Theoretical work on the transport behavior of non-spherical molecules was pioneered by the work of Debye¹ and Perrin^{2,3}. Brownian motion of a rotational ellipsoid in a viscous solvent is described in terms of a partial differential equation coupling rotational and translational diffusion (see also Ref. 4). The central quantity is $\rho(\mathbf{r}, \mathbf{u}, t; \mathbf{r}', \mathbf{u}', 0)$, the probability to find a molecule with center of mass (CMS) position \mathbf{r} and orientation \mathbf{u} at time t , given that its CMS position is \mathbf{r}' and its orientation is \mathbf{u}' at time $t = 0$. Its dynamical evolution is governed by the following translational-rotational diffusion equation, first introduced by Perrin^{2,3}:

$$\partial_t \rho(\mathbf{r}, \mathbf{u}, t; \mathbf{r}', \mathbf{u}', 0) = \left[-D_R \hat{L}^2 + D_{\parallel} (\nabla_{\mathbf{r}} \cdot \mathbf{u})^2 + D_{\perp} (\nabla_{\mathbf{r}}^2 - (\nabla_{\mathbf{r}} \cdot \mathbf{u})^2) \right] \rho(\mathbf{r}, \mathbf{u}, t; \mathbf{r}', \mathbf{u}', 0). \quad (1)$$

Here \mathbf{u} denotes the orientation of the symmetry axis of the molecule. The operator \hat{L}^2 is the familiar angular momentum operator. It describes rotational diffusion, D_R being the rotational diffusion constant. The usual Laplacian has been decomposed into directions parallel and perpendicular to the particle orientation, with parallel and perpendicular diffusion constants D_{\parallel} and D_{\perp} respectively.

Transport coefficients may be calculated using the Kirkwood-Riseman theory⁵ for rod-like molecules in solution. Broersma⁶ computes the rotational and isotropic translational diffusion coefficients approximately for long cylinders with no stick boundary conditions. Rods with capped hemispheres at the ends have also been considered^{7,8}. Alternatively the rods are composed of spherical hydrodynamic subunits^{9,10,11} with each sphere interacting with the other spheres via hydrodynamic interactions. The resulting transport coefficients obey the Stokes-Einstein relation, i.e. both the rotational and the translational diffusion constant are inversely proportional to the solvent viscosity. Transport properties of nonspherical molecules have also been computed using kinetic theory^{12,13,14,15}.

In polymer physics, the transport behavior of rod-like macromolecules has been investigated where anisotropic translational diffusion and the coupling of rotational and translational diffusion is most pronounced. The coupling of rotational and translational diffusion can be detected experimentally by depolarized light scattering. Dynamic light scattering from cylindrically symmetric rigid particles has been discussed by Aragon and Pecora^{16,17,18}. If only autocorrelations are included, the intensity of scattered light is proportional to the

intermediate scattering function

$$S(\mathbf{k}, t) = \frac{1}{N} \sum_{i=1}^N \langle \alpha^{(i)}(0) \alpha^{(i)}(t) e^{i\mathbf{k}(\mathbf{r}^i(t) - \mathbf{r}^i(0))} \rangle$$

$$\text{with } \alpha^{(i)} = \sum_{\nu, \mu=1}^3 n_{\nu}^{\text{inc}} \alpha_{\nu\mu}^{(i)} n_{\mu}^{\text{fin}}.$$

Here \mathbf{k} is the wave vector and $\alpha_{\nu\mu}^{(i)}$ is the polarizability tensor of particle i and $\mathbf{n}^{\text{inc}}(\mathbf{n}^{\text{fin}})$ denotes the polarization vector of the incident (scattered) light. Aragon and Pecora have solved the Perrin equation, allowing for a comparison of the theoretical predictions of the Perrin equation and the measured intensities. If the polarization of the incident and scattered light are orthogonal, then the scattering intensity is proportional to

$$S(\mathbf{k}, t) \sim \frac{1}{N} \sum_{i=1}^N \langle (\mathbf{u}_i(0) \cdot \mathbf{u}_i(t))^2 e^{i\mathbf{k}(\mathbf{r}^i(t) - \mathbf{r}^i(0))} \rangle \quad (2)$$

If the average over orientation and position is factorized, the intermediate scattering function decay with a rate $\Gamma = 6D_R + D_{\text{iso}}k^2$. The factorizing assumption, however, is valid only if the respective decay rates for orientational und positional degrees of freedom differ sufficiently. This is usually the case as long as $D_R \gg D_{\text{iso}}k^2$, which is guaranteed for small wave vectors. Hence translational and rotational diffusion coefficients can and have been obtained from polarized light scattering experiments^{19,20,21}, however the experiments are difficult due to low intensities of the scattered light²². Since rotational and lateral motions of a rod-like molecule are usually studied in light scattering experiments for $kL \geq 1$, where L is the rod length²², the factorizing assumption is bound to break down and coupling of translational and rotational diffusion will become important.

Even though the Perrin equation was originally formulated for the Brownian motion of a rodlike macromolecule in solution, it is usually thought to be applicable to the motion of a tagged rod in a fluid of otherwise identical rods. These systems have been simulated in the limit that the diameter of the rods goes to zero. Frenkel and Maguire²³ suggested an algorithm for the dynamics of hard needles and furthermore computed the autocorrelation of the linear velocity and the angular velocity in the Enskog approximation. The latter breaks down when the density ρ_0 is sufficiently high, such that the tagged rod cannot rotate unless other rods move out of the way. This so called semidilute transition density was estimated to be²⁴ $\rho_0 = \frac{N}{V}L^3 \sim 70$. Here N denotes the total number of rods of length L

confined to a volume V . For larger densities the rotational diffusion constant $D_R \sim \rho_0^{-2}$, as first suggested by Doi and Edwards with help of a scaling argument²⁵. They argue that rotational diffusion of a rod can be described by a random walk, so that the rotational diffusion constant is given by the product of the jump frequency, ν , and the average step size squared: $D_R = \nu(a/L)^2$. In the semidilute regime the jump frequency is $\nu \sim D_{\parallel}/L^2$ and the step size is $(a/L) \sim 1/\rho_0$, leading to the above scaling of D_R with density. A similar scaling argument has been formulated for the transverse diffusion coefficient. The inverse of the jump frequency ν can also be interpreted as the disentanglement time, or within the reptation model as the time needed for the breakup of the tube, confining the test rod. On time scales of order $1/\nu$ the rod can diffuse in the transverse direction by an amount a , giving rise to $D_{\perp} \sim a^2\nu \sim \rho_0^{-2}$. Such a scaling has been derived by Szamel and Schweizer^{26,27} within a dynamic mean field theory for self and tracer diffusion. They neglect rotational motion of the rods and close the hierarchy of dynamical distribution functions on the two particle level.

In this work, we discuss the microscopic dynamics of a gas of infinitely thin needles as a minimal model for rod-like macromolecules. An approximate kinetic theory is derived which allows us to determine the time delayed autocorrelation function of a tagged particle's density with a given orientation \mathbf{u} . We derive a hydrodynamic equation for this autocorrelation function from the microscopic collisional dynamics and examine the validity of the phenomenological Perrin equation in the limit of small wave vectors $kL \ll 1$. In fact, differences with the Perrin theory are found. In particular, meaningful anisotropic diffusion constants D_{\parallel} and D_{\perp} can only be obtained in the limit of high densities. In contrast to the Perrin theory we include the free motion of the particles in the microscopic theory, giving rise to ballistic behavior at short times. In addition to smooth needles, we consider rough needles²⁸, which allow for a change of the relative tangential velocity in a collision. The results, however, are qualitatively the same as for smooth needles.

The outline of the paper is as follows. In Sec. II we analyse the solutions of the Perrin equation following Aragon and Pecora. In particular we discuss anisotropic diffusion with help of the mean square displacement parallel and perpendicular to the rod's orientation. In Sec. III we analyse binary collisions of two hard needles and introduce a Pseudo Liouville operator for the time evolution of a gas of hard needles. Subsequently (Sec. IV) we apply the projection operator formalism of Mori and Zwanzig to the correlation function of interest,

which is thereby represented as a continued fraction. The formalism is applied to the density of a tagged particle with given orientation, i.e. $\rho(\mathbf{r}, \mathbf{u})$, in Sec. V. In Sec. VC we describe numerical simulations. The results of a truncation of the continued fraction are presented and compared with the simulation results in Sec. VI. We conclude with a discussion and outlook in Sec. VII.

II. ANALYSIS OF THE PERRIN EQUATION

In this section we review the predictions of the Perrin equation, Eq. (1), as discussed in Refs. 16,17,18, with particular emphasis on anisotropic diffusion. We do not present any new results, instead we want to familiarize the reader with this classic phenomenological theory. Later on, we will compare this theory with our kinetic theory, which is based on a microscopic dynamic model.

The first step in the solution of the Perrin equation is a Fourier transform with respect to the spatial coordinates

$$\tilde{\rho}(\mathbf{k}, \mathbf{u}, \mathbf{u}'; t) = \int d^3r e^{i\mathbf{k}\mathbf{r}} \rho(\mathbf{r}, \mathbf{u}, t; \mathbf{r}', \mathbf{u}', 0) \quad (3)$$

where we have assumed spatial homogeneity. The Fourier transformed function is the solution of

$$\partial_t \tilde{\rho}(\mathbf{k}, \mathbf{u}, \mathbf{u}', t) = [-D_R \hat{L}^2 - k^2 D_\perp - (D_\parallel - D_\perp)(\mathbf{k} \cdot \mathbf{u})^2] \tilde{\rho}(\mathbf{k}, \mathbf{u}, \mathbf{u}', t). \quad (4)$$

It is convenient to choose a coordinate frame $\mathbf{k} = k\hat{\mathbf{z}}$ with $k = |\mathbf{k}|$, so that the unit vector \mathbf{u} is specified by a polar angle ϕ and $\eta = \mathbf{k} \cdot \mathbf{u}/(k)$. In terms of ϕ and η the angular momentum operator is given explicitly by:

$$\hat{L}^2 = -\frac{\partial}{\partial \eta}(1 - \eta^2)\frac{\partial}{\partial \eta} - \frac{1}{1 - \eta^2}\frac{\partial^2}{\partial \phi^2} \quad (5)$$

Provided $\gamma^2 := (D_\parallel - D_\perp)k^2/D_R > 0$, the right hand side of Eq. (4) can be identified with the anisotropic Laplacian, whose eigenfunctions, $S_{m,l}(\gamma, \eta)e^{im\phi}$, are known and expressed in terms of the prolate spheroidal wavefunctions $S_{lm}^{29,30}$. The latter solve the equation

$$\left(-\frac{d}{d\eta}(1 - \eta^2)\frac{d}{d\eta} + \frac{m^2}{1 - \eta^2} + \gamma^2\eta^2\right) S_{lm}(\gamma, \eta) = \lambda_{lm}(\gamma^2) S_{lm}(\gamma, \eta) \quad (6)$$

with eigenvalues

$$\lambda_{lm}(\gamma^2) = l(l+1) + \frac{2l(l+1) - 2m^2 - 1}{(2l-1)(2l+3)}\gamma^2 + \mathcal{O}(\gamma^4) \quad (7)$$

We are interested in diffusion and hence consider only long wavelength phenomena, so that it suffices to keep terms up to and including $\mathcal{O}(\gamma^2)$.

The full solution of the Perrin equation can then be written in terms of the eigenfunctions

$$\tilde{\rho}(\mathbf{k}, \mathbf{u}, \mathbf{u}', t) = \frac{1}{8\pi^2} \sum_{m=0}^{\infty} \sum_{l=m} S_{lm}(\gamma, \eta) S_{lm}(\gamma, \eta') e^{im\phi} e^{-im\phi'} e^{-\Gamma_{lm}(\gamma^2)t} \quad (8)$$

such that the eigenvalues determine the relaxation rates according to $\Gamma_{lm}(\gamma^2) = D_{\perp}k^2 + D_R\lambda_{lm}(\gamma^2)$.

The anisotropic diffusive behaviour can be analysed and has been discussed in the literature in terms of the mean square displacement. We define the displacement $\Delta\mathbf{r}(t) := \mathbf{r}_0(t) - \mathbf{r}_0(0)$ and compute its projection on the initial orientation $\Delta r_{\parallel}(t) := \Delta\mathbf{r}(t) \cdot \mathbf{u}_0(0)$ as well as perpendicular to it $\Delta r_{\perp}(t) := \Delta\mathbf{r}(t) - \mathbf{u}_0(0)\Delta\mathbf{r}(t) \cdot \mathbf{u}_0(0)$. The Perrin equation predicts

$$\langle (\Delta r_{\parallel}(t))^2 \rangle = 2D_{\text{iso}}t + \frac{2(D_{\parallel} - D_{\perp})}{9D_R} (1 - e^{-6D_R t}) \quad (9)$$

$$\langle (\Delta r_{\perp}(t))^2 \rangle = 4D_{\text{iso}}t - \frac{2(D_{\parallel} - D_{\perp})}{9D_R} (1 - e^{-6D_R t}). \quad (10)$$

Analysing the short time behaviour one finds *anisotropic* diffusion, $\langle (\Delta r_{\parallel}(t))^2 \rangle \sim 2D_{\parallel}t$ and $\langle (\Delta r_{\perp}(t))^2 \rangle \sim 4D_{\perp}t$, such that in general the diffusive motion parallel to the initial orientation is faster than perpendicular to it. The asymptotic long time behaviour is again diffusive with, however, an *isotropic* diffusion constant $D_{\text{iso}} = (D_{\parallel} + 2D_{\perp})/3$. The crossover is determined by the rotational diffusion constant D_R , such that for $6D_R t \gg 1$ the initial orientation has been forgotten and diffusion is completely isotropic.

The above discussion already indicates that it might be difficult to detect anisotropic diffusion, since it is not the true asymptotic long time behaviour and, on the other hand, we expect ballistic motion for short times which is not accounted for in the Perrin equation. Hence the anisotropic diffusion on intermediate timescales will be superimposed by a crossover to ballistic motion on short time scales and isotropic diffusion on long time scales. Only if the density is sufficiently high, so that the time for rotation of the molecule is large, do we expect to see a clear separation of the two diffusive regimes.

Several attempts have been made to detect anisotropic diffusion from velocity autocorrelations. For isotropic diffusion there is a simple relation, connecting the asymptotic behaviour of the mean square displacement with the velocity autocorrelation, integrated over time. For anisotropic diffusion $\langle(\Delta r_{\parallel}(t))^2\rangle$ is *not* simply related to the autocorrelation of $v_{\parallel}(t) = \mathbf{v}(t) \cdot \mathbf{u}(0)$, as noted in Ref. 24.

III. DYNAMICS OF HARD NEEDLES

A. Collision rules

The phase space of needles is specified by the needles' translational and angular velocities \mathbf{v}_i , $\boldsymbol{\omega}_i$ and their center of mass positions \mathbf{r}_i and orientations \mathbf{u}_i , with $i = 0 \dots N$. The needles have length L , mass m and moment of inertia I . Given two needles, labeled 0 and 1, their orientations define a plane E_{01} whose normal vector is given by (see Fig. 1):

$$\mathbf{u}_{\perp} = \frac{\mathbf{u}_0 \times \mathbf{u}_1}{|\mathbf{u}_0 \times \mathbf{u}_1|} \quad (11)$$

The three vectors \mathbf{u}_0 , \mathbf{u}_{\perp} and

$$\mathbf{u}_0^{\perp} = \frac{\mathbf{u}_1 - (\mathbf{u}_0 \cdot \mathbf{u}_1)\mathbf{u}_0}{\sqrt{1 - (\mathbf{u}_0 \cdot \mathbf{u}_1)^2}}, \quad (12)$$

define a local orthonormal frame which is convenient for our calculations. For \mathbf{u}_1^{\perp} there is an analogous expression if one permutes indices 0 and 1 in the last equation. Let $\mathbf{r}_{01} = \mathbf{r}_0 - \mathbf{r}_1$ be the CMS distance between two needles, which may be decomposed into a component perpendicular $\mathbf{r}_{01}^{\perp} = (\mathbf{r}_{01} \cdot \mathbf{u}_{\perp})\mathbf{u}_{\perp}$ and parallel $\mathbf{r}_{01}^{\parallel} = s_{01}\mathbf{u}_0 - s_{10}\mathbf{u}_1$ to E_{01} ³¹. The parameters s_{ij} are determined from

$$s_{ij} = -\frac{\mathbf{r}_{ij} \cdot \mathbf{u}_j^{\perp}}{(\mathbf{u}_i \cdot \mathbf{u}_j^{\perp})} \quad (13)$$

Note that $\mathbf{u}_1^{\perp} = -\sqrt{1 - (\mathbf{u}_0 \cdot \mathbf{u}_1)^2}\mathbf{u}_0 + (\mathbf{u}_0 \cdot \mathbf{u}_1)\mathbf{u}_0^{\perp}$.

Let us recall the general collision rules for hard needles (see e.g. Ref. 32, with the coefficient of the normal restitution $\epsilon = 1$ and the coefficient of tangential restitution $\beta = \pm 1$). The relative velocity of the contact points is given by $\mathbf{V} = \mathbf{v}_0 - \mathbf{v}_1 + s_{01}\dot{\mathbf{u}}_0 - s_{10}\dot{\mathbf{u}}_1$ and can be decomposed with respect to the orthonormal frame $(\mathbf{u}_{\perp}, \mathbf{u}_0^{\perp}, \mathbf{u}_0)$ according to $\mathbf{V} = x\mathbf{u}_{\perp} + y\mathbf{u}_0^{\perp} + z\mathbf{u}_0$. The normal and tangential component of the relative velocity after

the collision (primed quantities) are given in terms of the respective components before the collision as follows:

$$(\mathbf{u}_\perp \cdot \mathbf{V}') = -(\mathbf{u}_\perp \cdot \mathbf{V}) \quad (14)$$

$$(\mathbf{u}_\perp \times \mathbf{V}') = -\beta(\mathbf{u}_\perp \times \mathbf{V}) \quad (15)$$

Here $\beta = -1$ for smooth needles, and $\beta = 1$ for totally rough needles, being the only values allowed by energy conservation. In terms of the particle's translational and angular velocities the collision rules are the following:

$$\begin{aligned} \mathbf{p}'_0 &= \mathbf{p}_0 + \Delta\mathbf{p} \\ \mathbf{p}'_1 &= \mathbf{p}_1 - \Delta\mathbf{p} \\ \boldsymbol{\omega}'_0 &= \boldsymbol{\omega}_0 + \frac{s_{01}}{I} \mathbf{u}_0 \times \Delta\mathbf{p} \\ \boldsymbol{\omega}'_1 &= \boldsymbol{\omega}_1 - \frac{s_{10}}{I} \mathbf{u}_1 \times \Delta\mathbf{p}. \end{aligned} \quad (16)$$

B. Perfectly smooth needles: $\beta = -1$

In this case, the translational momentum transfer occurs only perpendicular to the plane E_{01} , and is given by $\Delta\mathbf{p} = \alpha\mathbf{u}_\perp$ with

$$\alpha = -m \frac{(\mathbf{u}_\perp \cdot \mathbf{V})}{1 + \left(\frac{m}{2I}(s_{01}^2 + s_{10}^2)\right)} \quad (17)$$

The temporal change of orientation $\dot{\mathbf{u}}_0$ is changed by a collision due to translational momentum transfer, $I \Delta\dot{\mathbf{u}}_0 = s_{01}\Delta\mathbf{p}$.

C. Perfectly rough needles: $\beta = 1$

Rough needles also allow for a momentum transfer in the directions \mathbf{u}_0 and \mathbf{u}_0^\perp :

$$\Delta\mathbf{p} = \alpha\mathbf{u}_\perp + \gamma_1\mathbf{u}_0 + \gamma_2\mathbf{u}_0^\perp. \quad (18)$$

The coefficients γ_1 and γ_2 are given by:

$$\gamma_1 = \frac{1 + \beta}{2} \frac{By - Cz}{AC - B^2} \quad (19)$$

$$\gamma_2 = \frac{1 + \beta}{2} \frac{Bz - Ay}{AC - B^2} \quad (20)$$

with

$$A = \frac{1}{m} + \frac{s_{10}^2}{2I}(1 - (\mathbf{u}_0 \cdot \mathbf{u}_1)^2) \quad (21)$$

$$B = -\frac{s_{10}^2}{2I}(\mathbf{u}_0 \cdot \mathbf{u}_1)\sqrt{1 - (\mathbf{u}_0 \cdot \mathbf{u}_1)^2} \quad (22)$$

$$C = \frac{1}{m} + \frac{s_{01}^2}{2I} + \frac{s_{10}^2}{2I}(\mathbf{u}_0 \cdot \mathbf{u}_1)^2 \quad (23)$$

and the variables y, z as defined above. The change of angular velocity is given by the expression:

$$\Delta \dot{\mathbf{u}}_0 = \frac{s_{01}}{I} (\alpha \mathbf{u}_\perp + \gamma_2 \mathbf{u}_0^\perp). \quad (24)$$

D. Liouville operator for hard needles

The time evolution of any function $A(\Gamma, t)$ on phase space $\Gamma = \{\mathbf{r}_i, \mathbf{u}_i, \mathbf{v}_i, \boldsymbol{\omega}_i\}$ is determined by the pseudo-Liouville operator $\mathcal{L}_+^{13,14}$

$$A(\Gamma, t) = \exp(i\mathcal{L}_+ t) A(\Gamma, 0), \quad t > 0 \quad (25)$$

The pseudo-Liouville operator \mathcal{L}_+ consists of two parts, $\mathcal{L}_+ = \mathcal{L}^0 + \mathcal{L}'_+$. The first part results from the Poisson bracket with the Hamiltonian of free translational motion and rotation, $i\mathcal{L}^0 = \{\mathcal{H}, \dots\}$. For N needles the Hamiltonian expressed in terms of generalized canonical momenta is given as follows:

$$\mathcal{H} = \sum_{i=1}^N \left(\frac{1}{2m} \mathbf{p}_{\mathbf{r}_i}^2 + \frac{1}{2I} p_{\theta_i}^2 + \frac{1}{2I \sin^2(\theta_i)} p_{\phi_i}^2 \right) \quad (26)$$

The second part of the pseudo-Liouville-operator, describing binary collisions, reads

$$i\mathcal{L}'_+ = \frac{1}{2} \sum_{i \neq j} \left| \frac{d}{dt} |\mathbf{r}_{ij}^\perp| \right| \theta \left(-\frac{d}{dt} |\mathbf{r}_{ij}^\perp| \right) \theta \left(\frac{L}{2} - |s_{ij}| \right) \theta \left(\frac{L}{2} - |s_{ji}| \right) \delta(|\mathbf{r}_{ij}^\perp| - 0^+) (b_{ij}^+ - 1). \quad (27)$$

Here $\theta(x)$ is the Heaviside step function. The factor $\left| \frac{d}{dt} |\mathbf{r}_{ij}^\perp| \right|$ accounts for the flux of approaching needles (therefore requiring the factor $\theta(-\frac{d}{dt} |\mathbf{r}_{ij}^\perp|)$). The following two step functions and the delta functions enforce the conditions $\frac{L}{2} > |s_{ij}|$, $\frac{L}{2} > |s_{ji}|$, and $|\mathbf{r}_{ij}^\perp| = 0^+$ for a collision, assuming no lateral extension of the needles. Finally b_{ij} , acting on a phase space function $A(\Gamma)$, replaces linear and angular momenta before a collision by those after collision according to the rules given in Eq. (16). One can equally consider the evolution backwards in time. The corresponding Liouville operator is given in Ref. 32.

IV. PROJECTION OPERATOR FORMALISM

In the following, autocorrelation functions of phase space functions or observables $A(\Gamma, t)$ will be calculated:

$$\begin{aligned}\Phi(t) &= \langle A^*(\Gamma, 0) A(\Gamma, t) \rangle \\ &= \langle A^*(\Gamma, 0) \exp(i\mathcal{L}_+ t) A(\Gamma, 0) \rangle\end{aligned}\tag{28}$$

The bracket $\langle \dots \rangle$ defines an average with respect to the canonical ensemble with weight $\propto \exp(-\mathcal{H}/T)$. A^* denotes the complex conjugate of A . For later purposes, the Laplace transform is defined as follows:

$$\Phi(z) = i \int_0^\infty dt e^{izt} \phi(t) = -\langle A^*(\Gamma, 0) \frac{1}{z + \mathcal{L}_+} A(\Gamma, 0) \rangle.\tag{29}$$

The function $\Phi(z)$ is analytic for $\text{Im}(z) > 0$.

Following Mori and Zwanzig we can represent the autocorrelation function in terms of a continued fraction, which is suited to an approximation by truncation. Let us denote the resolvent in Eq. (29) by $\mathcal{R} = (\mathcal{L}_+ + z)^{-1}$ and define a scalar product of two dynamic variables A and B via the equilibrium expectation value as $(A|B) := \langle A^* B \rangle$. The Laplace transform of the autocorrelation can then be written as a matrix element of the resolvent $\Phi(z) = -(A|(z + \mathcal{L}_+)^{-1} A)$.

The idea behind the Mori Zwanzig formalism is to consider explicitly the dynamic evolution in a subspace of dynamic variables and treat the dynamics of the remaining variables in a simple approximation. The crux of the matter is to choose the right subspace. Popular candidates are the conserved quantities, which are special because of their long relaxation times in the hydrodynamic limit. The fast degrees of freedom are then approximated by a single relaxation time, similar in spirit to the single collision time approximation of the Boltzmann equation. We shall in the following consider the subspace spanned by $\rho(\mathbf{r}, \mathbf{u})$, but first review the general formalism.

We consider a set of dynamic variables $\{A_i\}$ with normalisation matrix $(\chi_0)_{ij} = (A_i|A_j) = \langle A_i^* A_j \rangle$. The projector onto the subspace spanned by the $\{A_i\}$ is given by $\hat{P}_0 = \sum_{i,j} |A_i\rangle (\chi_0^{-1})_{ij} \langle A_j|$. The orthogonal projector is denoted by $\hat{Q}_0 = 1 - \hat{P}_0$. Following the Mori-Zwanzig formalism we obtain an equation for the correlation functions $\Phi_{ij}(z) = -(A_i|(z + \mathcal{L}_+)^{-1} A_j)$. In matrix notation it reads

$$(z + \Omega_0 \chi_0^{-1} + M_0(z) \chi_0^{-1}) \Phi(z) = -\chi_0\tag{30}$$

with $(\Omega_0)_{ij} = (A_i|\mathcal{L}_+A_j)$ and the memory kernel

$$(M_0)_{ij}(z) = -(A_i|\mathcal{L}_+\hat{Q}_0(z + \hat{Q}_0\mathcal{L}_+\hat{Q}_0)^{-1}\hat{Q}_0\mathcal{L}_+A_j). \quad (31)$$

Since the memory kernel is again a matrix element of a modified resolvent taken with the state $B_i = \hat{Q}_0\mathcal{L}_+A_i$, we can iterate the procedure, thereby representing the autocorrelation as a continued fraction. We define a second projector $\hat{P}_1 = \sum_{ij} |B_i)(\chi_1^{-1})_{ij}(B_j|$ and $\hat{Q}_1 = 1 - \hat{P}_1$ and apply the same procedure to $M_0(z)$,

$$(z + \Omega_1\chi_1^{-1} + M_1(z)\chi_1^{-1}) M_0(z) = -\chi_1, \quad (32)$$

with $(\chi_1)_{ij} = (B_i|B_j)$, $(\Omega_1) = (B_i|\mathcal{L}_+B_j)$ and a second memory kernel $M_1(z)$.

In principle this procedure can be iterated an arbitrary number of times. However the computation of the static expectation values χ_i and Ω_i becomes increasingly complicated, so that one usually truncates the continued fraction after one or two steps. In the case of hard core interactions the “restoring forces” Ω_i are in general imaginary, because the Liouville operator is non hermitean. Hence even a truncation of the continued fraction with $M_1 = 0$ – the approximation scheme that will be adopted in this paper – will give rise to damping effects. This is in contrast to differentiable potentials with a Hermitean Liouville operator.

V. CORRELATIONS OF COUPLED DENSITY ORIENTATION FLUCTUATIONS

A. Observable and matrix elements

We are interested here in the anisotropic motion of a tagged rod-like macromolecule. In particular we want to compute the anisotropic diffusion constants D_\perp and D_\parallel as well as the rotational diffusion constant D_R (see Eq.(1)) from a kinetic theory approach. The dynamic variables of interest are thus the density of a tagged particle $\rho(\mathbf{r}, \mathbf{u}) = \delta(\mathbf{r} - \mathbf{r}_0)\delta(\mathbf{u} - \mathbf{u}_0)$ for all orientations \mathbf{u} . It is convenient to consider its Fourier transform $\rho(\mathbf{k}, \mathbf{u}) = e^{-i\mathbf{k}\mathbf{r}_0}\delta(\mathbf{u} - \mathbf{u}_0)$ and compute the matrix of correlation functions

$$\Phi_{\mathbf{u}, \mathbf{u}'}(\mathbf{k}, z) = -(\rho(\mathbf{k}, \mathbf{u})|(z + \mathcal{L}_+)^{-1}\rho(\mathbf{k}, \mathbf{u}')) \quad (33)$$

where the orientation vector \mathbf{u} is the “matrix subscript”. Actually \mathbf{u} is continuous, so that the matrix equations turn into integral equations. To apply the formalism of Mori and

TABLE I: Geometrical factors c_{\parallel} , c_{\perp} and c_R for homogeneous rods ($W = 6$) and “dumbbells” ($W = 2$), rounded to 3 decimal places.

	smooth rods		rough rods	
	$W = 6$	$W = 2$	$W = 6$	$W = 2$
c_{\parallel}	0	0	10.631	10.202
c_{\perp}	7.253	8.626	11.802	13.390
c_R	0.544	0.684	0.871	1.058

Zwanzig, we identify

$$A_{\mathbf{u}} = \rho(\mathbf{k}, \mathbf{u}) = e^{-i\mathbf{k}\mathbf{r}_0} \delta(\mathbf{u} - \mathbf{u}_0). \quad (34)$$

We consider two steps in the continued fraction and only discuss the simplest approximations $M_1 = 0$. As will be shown below, the resulting correlation function $\Phi_{\mathbf{u}, \mathbf{u}'}(\mathbf{k}, z)$ has the right hydrodynamic limit. It furthermore accounts for free particle motion approximately. More elaborate approximations as well as the effects of further steps in the continued fraction will be discussed in the conclusions.

The computation of susceptibilities χ_i and “restoring forces” Ω_i is straightforward but cumbersome and hence delegated to appendix A (see also Refs. 33,34). The results of this calculation are

$$(\chi_0)_{\mathbf{u}, \mathbf{u}'} = (A_{\mathbf{u}} | A_{\mathbf{u}'}) = (4\pi)^{-1} \delta(\mathbf{u} - \mathbf{u}') \quad (35)$$

$$(\Omega_0)_{\mathbf{u}, \mathbf{u}'} = (A_{\mathbf{u}} | \mathcal{L}_+ A_{\mathbf{u}'}) = 0 \quad (36)$$

$$(\chi_1)_{\mathbf{u}', \mathbf{u}} = (\dot{A}_{\mathbf{u}} | \dot{A}_{\mathbf{u}'}) = \frac{1}{4\pi} \left(\frac{T}{m} k^2 + \frac{T}{I} \hat{L}^2 \right) \delta(\mathbf{u} - \mathbf{u}') \quad (37)$$

$$(\Omega_1)_{\mathbf{u}', \mathbf{u}} = (\dot{A}_{\mathbf{u}} | \mathcal{L}_+ \dot{A}_{\mathbf{u}'}) = i \frac{n_0}{8\pi^{5/2}} \left(\frac{T}{m} \right)^{3/2} \left[c_{\parallel} L^2 (\mathbf{k} \cdot \mathbf{u})^2 + c_{\perp} L^2 (k^2 - (\mathbf{k} \cdot \mathbf{u})^2) + 4W^2 c_R \hat{L}^2 \right] \delta(\mathbf{u}' - \mathbf{u}). \quad (38)$$

Here the angular momentum operator is defined as usual (see Eq. (5)). The constants c_{\parallel} , c_{\perp} , and c_R are geometrical factors specific to needles, depending on the dimensionless ratio $W = mL^2/(2I)$. They are defined in App. B and their numerical values are listed in Tab. I for $W = 6$, corresponding to homogeneous rods, and $W = 2$, corresponding to rods whose mass is concentrated at the endpoints (“dumbbells”).

B. The correlation function

Given the matrix elements obtained above, we proceed to find a solution for $\Phi_{\mathbf{u}, \mathbf{u}'}(\mathbf{k}, z)$ within the approximation $M_1 = 0$. Since Ω_0 and χ_0 are trivial quantities, we will concentrate on Ω_1 and χ_1 and drop the subscript 1 from now on for notational simplicity. Additionally, we absorb a factor of $1/\chi_0 = 4\pi$ by defining $\varphi = 4\pi\Phi$. Multiplying Eq. (30) from the left by $(z + \Omega\chi^{-1})$ (and using Eq. (32)), we are then left with the matrix equation (w.r.t. \mathbf{u} and \mathbf{u}')

$$(z^2 + z\Omega\chi^{-1} - 4\pi\chi)\varphi = -(z + \Omega\chi^{-1}) \quad (39)$$

What is an appropriate set of functions to represent φ in? The matrix χ is diagonal in the eigenfunctions of the isotropic Laplacian, i.e. the spherical harmonics. The matrix Ω is diagonal in the eigenfunctions of the anisotropic Laplacian, denoted by $y_{lm}(ic, \mathbf{u})$ and related to the *oblate* spheroidal polynomials (or *oblate* spheroidal wave functions) $S_{lm}(ic, \eta)$ in the same way as the spherical harmonics are related to the associated Legendre functions,

$$y_{lm}(ic, \mathbf{u}) = y_{lm}(ic, \eta, \phi) = \frac{1}{\sqrt{2\pi}} S_{lm}(ic, \eta) e^{im\phi}, \quad (40)$$

with $\eta = \mathbf{u} \cdot \mathbf{k}/k$. The properties of spheroidal wave functions are discussed in App. C.

As will become evident below, we do not need to keep the dependence on the azimuthal angles ϕ and ϕ' in Eq. (39) and integrate the equation over these variables to obtain

$$\int d\eta'' (z^2 + z\Omega\chi^{-1} - 4\pi\chi)_{\eta\eta''} \varphi_{\eta''\eta'} = -(z + \Omega\chi^{-1})_{\eta\eta'}. \quad (41)$$

Here $\varphi_{\eta\eta'}$ is defined as

$$\varphi_{\eta\eta'} = \frac{1}{2\pi} \int d\phi \int d\phi' \varphi_{\mathbf{u}\mathbf{u}'} \quad (42)$$

and analogously

$$\begin{aligned} \Omega_{\eta\eta'} &= \sum_l \Omega_l S_{l0}(ic, \eta) S_{l0}(ic, \eta') \\ \chi_{\eta\eta'} &= \sum_l \chi_l S_{l0}(0, \eta) S_{l0}(0, \eta'). \end{aligned} \quad (43)$$

The expansion coefficients are given by

$$\begin{aligned} \Omega_l &= i\kappa \left(\frac{c_\perp k^2 L^2}{4W^2 c_R} + \lambda_{l0}(-c^2) \right), \\ \chi_l &= \frac{1}{4\pi} \left(\frac{T}{m} k^2 + \frac{T}{I} l(l+1) \right), \end{aligned} \quad (44)$$

with $c^2 = \frac{c_\perp - c_\parallel}{4W^2 c_R} (Lk)^2$ and $\kappa = \frac{\rho_0 W^2 c_R}{2\pi L^3} \left(\frac{T}{\pi m}\right)^{3/2}$.

In App. D we show how to diagonalize $\varphi_{\eta\eta'}$ perturbatively for $k \rightarrow 0$. For the time being, however, we choose the set $S_{l0}(0, \eta) \propto P_l(\eta)$ to expand $\varphi_{\eta\eta'}$ as

$$\varphi_{\eta\eta'} = \sum_{l,l'} \varphi_{ll'} S_{l0}(0, \eta) S_{l'0}(0, \eta'). \quad (45)$$

In particular, we will later need the matrix elements φ_{00} and φ_{20} , which are calculated from the diagonalized φ in App. D. The result is

$$\varphi_{00} = -\frac{z + \chi_0^{-1} \Omega_0}{z^2 + z\chi_0^{-1} \Omega_0 - 4\pi\chi_0} \quad (46)$$

$$\begin{aligned} \varphi_{20} &= 4\pi \frac{c^2}{9\sqrt{5}} \frac{-\Omega_2}{(z^2 + z\chi_0^{-1} \Omega_0 - 4\pi\chi_0) (z^2 + z\chi_2^{-1} \Omega_2 - 4\pi\chi_2)} \\ &= \varphi_{02} + \mathcal{O}(k^4), \end{aligned} \quad (47)$$

where only terms up to and including $\mathcal{O}(k^2)$ have been retained.

C. Numerical simulations

We have performed simulations of the system of hard rods using an event-driven algorithm as described in Ref. 35 (with no inelasticity). We used system sizes of $N = 800$ to $N = 2048$ and densities between $\rho_0 = 0.25$ and $\rho_0 = 100$. For the most part we used homogeneous rods with $W = 6$. The results of the simulations will be discussed below along with the theoretical ones.

VI. RESULTS

In this section we are going to discuss the results of the approximate kinetic theory obtained by setting $M_1 = 0$. One might expect that our theory reduces to the diffusion equation of Perrin in the limit of small wave numbers $kL \ll 1$ and long times. However, such a straightforward limit does not exist as we will show below.

There are two special cases where the comparison between microscopic theory and the Perrin equation is straightforward. One case concerns purely rotational motion. We show that the theory predicts a crossover as a function of density from weakly damped free rotations to rotational diffusion. We furthermore obtain explicit expressions for the rotational

diffusion constant of the Perrin theory as well as for the damping of the free rotations. The other important case which allows for direct comparison with the Perrin theory is purely translational motion, where we recover the isotropic diffusion constant.

The third and most interesting case, however, concerns the coupling of translational and rotational degrees of freedom. The comparison with the Perrin diffusion equation is not directly evident. In fact, we derive – within kinetic theory – the full time dependence of the mean square displacements of a tagged rod parallel and perpendicular to its initial orientation. We then compare our expressions to the corresponding ones obtained from the Perrin theory. An important problem arising in the analysis is the appearance of short time scales present in the kinetic theory which are not easily decoupled from the long-time behavior. One would like to map the latter to the Perrin diffusion equation which involves only long-time diffusive time scales. Even within the Perrin theory, the anisotropic translational motion characterized by the diffusion constants D_{\parallel} and D_{\perp} is only perceptible on small times (compared to the rotational diffusion time) before the anisotropy is hidden by the long-time isotropic translational diffusion of the center of mass of the tagged rod. On the side of kinetic theory, the time interval for anisotropic diffusion to be observed is bounded from below by ballistic motion which is isotropic a priori. We comment on this point in more detail below when comparing our analytical results with simulations.

A. Rotational diffusion

We first discuss purely rotational motion, as obtained from the results of Sec. V by setting $\mathbf{k} = 0$. In order to compare with simulation results later on we focus on the Fourier transform $\varphi(\omega)$ instead of the Laplace transform $\varphi(z)$ of the correlation function. Since in the time domain $\varphi(t)$ is a real symmetric function, the Fourier and Laplace transforms are related via $\varphi(\omega) = 2\text{Im}(\varphi(z = \omega + i0))$ where ω is real.

The correlation function for $\mathbf{k} = 0$ is diagonal in the angular momentum quantum numbers and is given by

$$\varphi_l(z) = -\frac{z^*|z + i\zeta|^2 - (z + i\zeta)\omega_l^2}{|z^2 - \omega_l^2|^2 + |z|^2\zeta^2 + 2\text{Im}(\zeta z^*(z^2 - \omega_l^2))} \quad (48)$$

with $\omega_l^2 = \frac{T}{I}l(l+1)$ and $\zeta = 4\pi\kappa\frac{I}{T}$. The Fourier transform is

$$\varphi_l(\omega) = 2\frac{\zeta\omega_l^2}{(\omega^2 - \omega_l^2)^2 + \omega^2\zeta^2}. \quad (49)$$

The correlation function Eq. (49) has two poles in the lower complex frequency plane at $\omega = -i\zeta/2 \pm \sqrt{(\omega_l^2 - \zeta^2/4)}$ and the corresponding complex conjugates in the upper half plane. It shows qualitatively different behaviour depending on the reduced density $\rho_0 = n_0 L^3$. For low density the poles have a nonzero real part, corresponding to weakly damped oscillatory motion of the rods:

$$\varphi_{ll}(t) = \frac{1}{\omega_l} \exp(-\zeta t/2) (\omega_l \cos(\omega_l t) + \zeta \sin(\omega_l t)) \quad (50)$$

The real part of the poles vanishes above a critical density $\rho_{\text{crit}}(l) = \left(l(l+1)\frac{8\pi^3}{c_R^2 W}\right)^{1/2}$ which depends on l . For large density the time dependent correlation function is a sum of two exponentials with the long relaxation time $\tau_{\text{long}}(l) = (D_R l(l+1))^{-1}$ and the short relaxation time $\tau_{\text{short}} = \zeta^{-1}$. The decay on long times corresponds to rotational diffusion and is in agreement with the Perrin theory. The rotational diffusion constant is given by

$$D_R = \frac{2\pi^{3/2}}{\rho_0 L c_R} \sqrt{\frac{T}{m}} \quad (51)$$

Our approximate theory does not describe the free particle limit $\rho_0 \rightarrow 0$ correctly. In particular the weakly damped oscillations acquire additional damping due to free particle motion (sometimes called motional narrowing). We discuss a simple way to account for these additional terms approximately.

If there are no interactions, the angular correlations are simply given by

$$\varphi_{ll}^0(t) = \langle P_l(\cos \omega t) \rangle_{\text{th}} = \int_0^\infty d\omega \, \omega \frac{I}{T} P_l(\cos \omega t) e^{-\frac{\omega^2 I}{2T}}. \quad (52)$$

For example for $l = 1$ (the case we will need below) the correlation function $\varphi_{11}^0(z)$ can be expressed in terms of the exponential integral function $E_1(z)$ ³⁶.

A simple way to incorporate free particle motion is the following. One represents the correlation function φ_{ll}^0 as a continued fraction with $\Omega = 0$ but $M \neq 0$ (see Eq. (30)),

$$\varphi_{ll}^0(z) = -\frac{1}{z - \frac{4\pi\chi_l}{z + M_l/\chi_l}}. \quad (53)$$

Then the memory kernel is expressed in terms of φ_{ll}^0 ,

$$z + M_l/\chi_l = 4\pi\chi_l \frac{\varphi_{ll}^0(z)}{z\varphi_{ll}^0(z) + 1}, \quad (54)$$

and can now substituted in the continued fraction for the interacting system. This procedure yields

$$\varphi_l(z) = -\frac{\frac{\Omega_l}{\chi_l}(z\varphi_l^0 + 1) + 4\pi\varphi_l^0\chi_l}{z\frac{\Omega_l}{\chi_l}(z\varphi_l^0 + 1) + 4\pi\chi_l}. \quad (55)$$

We now compare the Fourier transform $\varphi_l(\omega) = 2\text{Im}(\varphi_l(z = \omega + i0))$ for the case $l = 1$, which corresponds to the correlation function $\varphi_{11}(t) = \langle \mathbf{u}_0(t) \cdot \mathbf{u}_0(0) \rangle$, with numerical simulations in Fig 2. Agreement is very good for small densities because the free particle limit has been incorporated. Our approximate theory also reproduces the crossover from damped oscillations, corresponding to a peak at finite frequency in the spectrum, to purely relaxational motion, characterized by a peak at zero frequency.

B. Translational dynamics

Next we discuss purely translational motion, obtained from the general results by setting $l = l' = 0$, i.e. by examining the correlation function φ_{00} as given in Eq. (46). Its Fourier transform is given by

$$\varphi_{00}(\omega) = 2\frac{(kv_{\text{th}})^2}{(\omega^2 - (kv_{\text{th}})^2)^2 + \xi^2\omega^2} \quad (56)$$

with $\xi = \nu \frac{c_{\parallel} + 2c_{\perp}}{(2\pi)^2}$. Here we have introduced the Enskog collision frequency $\nu = \frac{2\rho_0}{3L} \sqrt{\frac{\pi T}{m}}$ and the thermal velocity $v_{\text{th}}^2 = T/m$.

The corresponding time dependent correlation function is the sum of two exponentials. The decay rate of the fast component, τ_0 , is determined by the collision rate according to $\tau_0^{-1} = \nu(c_{\parallel} + 2c_{\perp})/(2\pi)^2$. The decay rate of the slow component is diffusive as it should be, due to particle number conservation. Since we consider translational motion only and consequently have set $l = 0$ in the equation of motion, we should recover the isotropic diffusion constant of the Perrin theory. The latter predicts $D_{\text{iso}} = (D_{\parallel} + 2D_{\perp})/3$. Comparison with the Perrin theory allows us to identify

$$D_{\text{iso}} = \frac{v_{\text{th}}^2}{\nu} \frac{(2\pi)^2}{c_{\parallel} + 2c_{\perp}} = \sqrt{\frac{T\pi}{m}} \frac{6\pi L}{\rho_0(c_{\parallel} + 2c_{\perp})}. \quad (57)$$

The ratio of the rotational to the isotropic translational diffusion constant is given in the Kirkwood-Riseman theory⁵ by $D_R/D_{\text{iso}} = 9/L^2$. Even though this theory is designed for a rodlike molecule in a solvent where hydrodynamic interactions are important, we do find

almost the same result for a melt of smooth needles with a homogeneous mass distribution: $D_R/D_{\text{iso}} = (c_{\parallel} + 2c_{\perp})/(3c_R L^2) = 8.89/L^2$ (see Tab. I). The ratio does depend on the mass distribution though and is different for smooth and rough rods.

In summary, our approximate kinetic theory correctly describes particle diffusion which dominates the long time decay of the translational correlation function. It yields an approximate expression for the isotropic diffusion constant, which is inversely proportional to the density ρ_0 . The decay of the nonconserved variables has been approximated by a single relaxation time, which is inversely proportional to the Enskog collision frequency.

C. Coupled translational and rotational dynamics: kinetic theory

1. From correlation functions to mean square displacements

Our next goal is to calculate the mean-square displacement of the tagged rod, decomposed into the directions parallel and perpendicular to its initial orientation $\mathbf{u}_0(0)$. We define the tensor

$$R_{\alpha\beta\gamma\delta} = \langle \Delta r_{\alpha}(t) \Delta r_{\beta}(t) u_{0\gamma}(0) u_{0\delta}(0) \rangle, \quad (58)$$

where $\Delta \mathbf{r}(t) = \mathbf{r}_0(t) - \mathbf{r}_0(0)$ is the displacement of the tagged rod. This tensor $R_{\alpha\beta\gamma\delta}$ is isotropic and symmetric under exchange of the indices α and β and also of γ and δ . These symmetries imply that there are only two independent tensor components R_1 and R_2 such that

$$R_{\alpha\beta\gamma\delta} = \delta_{\alpha\beta} \delta_{\gamma\delta} R_1 + (\delta_{\alpha\gamma} \delta_{\beta\delta} + \delta_{\alpha\delta} \delta_{\beta\gamma}) R_2. \quad (59)$$

In order to calculate $R_{\alpha\beta\gamma\delta}$, we express it in terms of the correlation function Φ ,

$$\begin{aligned} R_{\alpha\beta\gamma\delta} &= -\frac{\partial^2}{\partial k_{\alpha} \partial k_{\beta}} \langle e^{i\mathbf{k} \cdot \Delta \mathbf{r}(t)} u_{0\gamma}(0) u_{0\delta}(0) \rangle \Big|_{\mathbf{k}=0} \\ &= -\frac{\partial^2}{\partial k_{\alpha} \partial k_{\beta}} \int d\mathbf{u} d\mathbf{u}' u'_{\gamma} u'_{\delta} \Phi_{\mathbf{u}\mathbf{u}'}(\mathbf{k}, t) \Big|_{\mathbf{k}=0}. \end{aligned} \quad (60)$$

The total mean-square displacement can easily be expressed in terms of this tensor as

$$\langle \Delta \mathbf{r}^2(t) \rangle = \sum_{\alpha\beta} R_{\alpha\alpha\beta\beta} = 9R_1 + 6R_2 = -\sum_{\alpha} \frac{\partial^2}{\partial k_{\alpha}^2} \int d\mathbf{u} d\mathbf{u}' \Phi_{\mathbf{u}\mathbf{u}'}(\mathbf{k}, t) \Big|_{\mathbf{k}=0} = -3 \frac{\partial^2}{\partial k^2} \varphi_{00} \Big|_{k=0} \quad (61)$$

(recall that Φ and φ are identical up to a factor of 4π). In the last step the derivatives become simpler since φ_{00} is only a function of k^2 (cf. Eq. (46)).

In terms of R_1 and R_2 the parallel mean-square displacement is given by (cf. Eq. (59))

$$\langle \Delta r_{\parallel}^2(t) \rangle = \sum_{\alpha\beta} R_{\alpha\beta\alpha\beta} = 3R_1 + 12R_2. \quad (62)$$

In order to evaluate this further, we need to know one more equation besides Eq. (61) to determine R_1 and R_2 . This is provided by

$$\begin{aligned} \sum_{\alpha} R_{\alpha\alpha\alpha\alpha} &= 3R_1 + 6R_2 = - \sum_{\alpha} \frac{\partial^2}{\partial k_{\alpha}^2} \int d\mathbf{u} d\mathbf{u}' (u'_{\alpha})^2 \Phi_{\mathbf{u}\mathbf{u}'}(\mathbf{k}, t) \Big|_{\mathbf{k}=0} \\ &= - \frac{\partial^2}{\partial k^2} \left(\frac{2}{\sqrt{5}} \varphi_{02} + \varphi_{00} \right) \Big|_{k=0}. \end{aligned} \quad (63)$$

Note that each term in the sum over α does not depend on α because of symmetry and the fact that φ_{00} and φ_{02} only depend on k^2 . Thus it suffices to evaluate the term with e.g. $\alpha = 3$.

Eqs. (61), (62), and (63) then result in

$$\langle \Delta r_{\parallel}^2(t) \rangle = - \frac{\partial^2}{\partial k^2} (\varphi_{00} + \sqrt{5} \varphi_{02}) \Big|_{k=0} \quad (64)$$

$$\langle \Delta \mathbf{r}_{\perp}^2(t) \rangle = - \frac{\partial^2}{\partial k^2} (2\varphi_{00} - \sqrt{5} \varphi_{02}) \Big|_{k=0}. \quad (65)$$

2. Anisotropic diffusion from kinetic theory

Given the expression derived above for the mean square displacement parallel and perpendicular to the initial orientation, the last step remaining is the calculation of the correlation functions $\varphi_{00}(k, t)$ and $\varphi_{20}(k, t)$ in the time domain from the corresponding expressions derived in the previous section for the Laplace transform (depending on z). Therefore, we need to analyse the poles of $\varphi_{00}(k, z)$ and $\varphi_{20}(k, z)$. The denominators of $\varphi_{00}(k, z)$ and $\varphi_{20}(k, z)$ consist of factors of the form $z^2 + \frac{\Omega_n}{\chi_n} z - 4\pi\chi_n$ ($n = 0, 2$). The two roots of each of these expressions are at

$$z_{n,\pm} = - \frac{\Omega_n}{2\chi_n} (1 \pm \sqrt{1 + 16\pi\chi_n^3/\Omega_n^2}). \quad (66)$$

While $\varphi_{00}(k, z)$ only contains the $n = 0$ factor and thus has the two poles $z_{0,\pm}$, $\varphi_{20}(k, z)$ has both the $n = 0$ and $n = 2$ factors and therefore has all four poles.

Given these poles, we can expand φ_{00} and φ_{20} from Eqs. (46) and (47) into partial fractions and carry out the inverse Laplace transforms. From Eqs. (64) and (65) we then get the mean-square displacements. Before we show the results of this straightforward but tedious calculation, we note that the long-time behavior on long length scales ($\mathbf{k} \rightarrow 0$) is determined by the pole or poles closest to the origin. Each pole $z_{n,\pm}$ corresponds to a timescale $1/(iz_{n,\pm})$ (provided $z_{n,\pm}$ is purely imaginary, see below). Inserting the values from Eq. (44) these timescales are (immediately setting $k = 0$ where possible)

$$\tau_0 = \frac{1}{iz_{0,+}} = D_{\text{iso}} \frac{m}{T} = \sqrt{\frac{m}{T}} \frac{6L\pi^{3/2}}{\rho_0(2c_{\perp} + c_{\parallel})} \quad (67)$$

$$\tau_1 = \frac{1}{iz_{2,+}} = \sqrt{\frac{m}{T}} \frac{2\pi^{3/2}L}{\rho_0 W c_R} \left(1 + \sqrt{1 - 48\pi^3/(\rho_0^2 W c_R^2)}\right)^{-1} \quad (68)$$

$$\tau_2 = \frac{1}{iz_{2,-}} = \sqrt{\frac{m}{T}} \frac{2\pi^{3/2}L}{\rho_0 W c_R} \left(1 - \sqrt{1 - 48\pi^3/(\rho_0^2 W c_R^2)}\right)^{-1} \quad (69)$$

$$\tau_3 = \frac{1}{iz_{0,-}} = \frac{1}{D_{\text{iso}} k^2}. \quad (70)$$

Generically, only one of these times is long, namely τ_3 , which is proportional to $1/k^2$. For large densities, however, τ_2 becomes proportional to the density and thus large, too. This indicates that, at least for high densities, there are *two* long time scales. The other two times scales, τ_0 and τ_1 , are short. The first one, τ_0 , is related to the Enskog collision time. The second one, τ_1 , is of the same order as τ_0 . For large densities it agrees with the short rotational timescale τ_{short} from Sec. VI A. It characterizes the crossover from free rotational motion to rotational diffusion.

After performing the inverse Laplace transforms, we find

$$\langle \Delta \mathbf{r}^2 \rangle = 6D_{\text{iso}} (t + \tau_0(\exp(-t/\tau_0) - 1)) \quad (71)$$

$$\langle \Delta r_{\parallel}^2 \rangle = \frac{1}{3} \langle \Delta \mathbf{r}^2 \rangle + \langle \Delta r_{\text{aniso}}^2 \rangle \quad (72)$$

$$\langle \Delta r_{\perp}^2 \rangle = \frac{2}{3} \langle \Delta \mathbf{r}^2 \rangle - \langle \Delta r_{\text{aniso}}^2 \rangle \quad (73)$$

where

$$\langle \Delta r_{\text{aniso}}^2 \rangle = -\frac{4\pi\kappa(c_{\perp} - c_{\parallel})L^2}{3W^2 c_R} \sum_{p=0}^3 \frac{e^{-it/\tau_p}}{\prod_{p' \neq p} (1/\tau_p - 1/\tau_{p'})} \Big|_{k=0}. \quad (74)$$

Due to the density dependence of Ω_2 the poles $z_{2,\pm}$ acquire a real part for *small* densities, such that the pole is no longer purely diffusive but oscillatory. Note, however, that the mean-square displacements are real quantities whether $z_{2,\pm}$ are purely imaginary (corresponding

to an exponential decay of the nonlinear part of the mean-square displacements) or not (corresponding to an oscillatory behavior).

The anisotropic mean square displacements calculated from kinetic theory have the following important characteristics:

- For short times $t \ll \tau_0$ one obtains ballistic behavior $2\langle\Delta r_{\parallel}^2(t)\rangle \simeq \langle\Delta \mathbf{r}_{\perp}^2(t)\rangle \simeq 2v_{\text{th}}^2 t^2$. The time τ_0 is identical to the fast timescale calculated in Sec. VIB.
- For long times $t \gg \tau_2$ the mean square displacements approach the isotropic center of mass diffusion behavior $2\langle\Delta r_{\parallel}^2(t)\rangle \simeq \langle\Delta \mathbf{r}_{\perp}^2(t)\rangle \simeq 4D_{\text{iso}}t$
- For large densities, the pole $z_{2,-}$ is given by

$$z_{2,-} \simeq -\frac{\Omega_2}{2\chi_2} \left(1 - 1 - 8\pi \frac{\chi_2^3}{\Omega_2^2} \right) = -6iD_R \quad (75)$$

with the rotational diffusion constant D_R given in Eq. (51). The timescale τ_2 is therefore $\tau_2 = (6D_R)^{-1} = \tau_{\text{long}}(l = 2)$ where τ_{long} is the long rotational timescale (see Sec. VIA). It also agrees with the crossover time from Perrin theory, see Eqs. (9) and (10).

- For intermediate times, when $\tau_0 \ll t \ll \tau_2$ (provided such an interval exists, which is only the case for high enough density), there is a linear (in t) regime in $\langle\Delta r_{\text{aniso}}^2\rangle$ which corresponds to *anisotropic diffusion*. The diffusion constants $D_{\perp} = D_{\text{iso}} - \frac{1}{2}\Delta D$ and $D_{\parallel} = D_{\text{iso}} + \Delta D$ in this regime can be calculated from Eq. (74), resulting in

$$\Delta D = \frac{2\pi\kappa(c_{\perp} - c_{\parallel})L^2}{3W^2c_R(1/\tau_2 - 1/\tau_1)(1/\tau_2 - 1/\tau_0)} \quad (76)$$

$$\xrightarrow{\rho_0 \rightarrow \infty} \frac{(c_{\perp} - c_{\parallel})L^2}{(2c_{\perp} + c_{\parallel})W} D_R$$

3. Anisotropic diffusion from simulations

The results of our analytic calculation are compared with the simulations in Figs. 3, 4 and 5 for homogeneous rods ($W = 6$) and in Fig. 6 for dumbbell molecules ($W = 2$).

The agreement between theory and simulations is very good for small densities $\rho_0 \leq 10$ but at these densities there is hardly any discernible anisotropy (see Fig. 3).

For higher densities an anisotropy window opens up between the parallel and perpendicular mean-square displacement curves. This is exemplified in Fig. 4. For densities above

≈ 20 the isotropic diffusion constants (slopes of the mean square displacements) *increase* with density in the simulation. This effect is well known^{23,24} and is due to enhanced parallel diffusion along a tube formed by surrounding particles. This involves correlated particle collisions and is thus not captured within our theory. Therefore the theory does not fit the data quantitatively but Fig. 4 shows that the anisotropy is very well captured qualitatively. But even though anisotropy is clearly present, it can (at these densities) not adequately be described by anisotropic diffusion constants since the anisotropy window is still small and within it, no convincing “straight line fit” appears possible. This is true for both theory and simulation.

Fig. 5 shows a direct comparison of theory and simulations of the mean-square displacements for densities $\rho_0 = 40$ and $\rho_0 = 100$. Here it becomes obvious that the isotropic diffusion constant is underestimated by the theory. The simulations at $\rho_0 = 100$ now very clearly show anisotropic diffusion with a well-defined perpendicular diffusion constant D_{\perp} . The parallel diffusion constant D_{\parallel} , on the other hand, is still not well defined even at this density.

The anisotropy becomes even more pronounced for dumbbell molecules with $W = 2$ at $\rho = 100$, which is shown in Fig. 6. The reason the effect is more pronounced for dumbbells lies in the W -dependence of the diffusion constants. While ΔD is proportional to $1/W$ (see Eq. (76)), D_{iso} is only weakly dependent on W through c_{\parallel} and c_{\perp} . Therefore anisotropic diffusion is more pronounced for smaller W .

VII. DISCUSSION AND OUTLOOK

Before we go into a discussion of the details of our results we will give a brief overview of our main findings. The aim of this paper is to gain some microscopic understanding of the transport properties of a gas of thin hard rods beyond the phenomenological Perrin equation. Purely rotational and translational dynamics of a tagged particle can be described by simple rotational or translational diffusion, in agreement with the Perrin equation, allowing us to calculate the rotational and isotropic translational diffusion constants. The motion of a tagged particle along and perpendicular to its original orientation shows marked anisotropies. The nature of the anisotropy is, however, very different from the one predicted by Perrin theory, at least for low and medium densities. This is confirmed by simulations. The

Perrin equation predicts anisotropies which can be described as anisotropic diffusion for all densities. In contrast, our results for low densities exhibit only a very drawn-out crossover from ballistic motion for short times to isotropic diffusion at long times with no intermediate regime which could be characterized as anisotropic diffusion. For medium densities $\rho_0 \approx 40$ such a regime begins to emerge; it is however still far from being well-defined. Even for densities $\rho_0 = 100$ where the mean-square displacement is clearly anisotropic, anisotropic *diffusion* is only seen in the perpendicular motion.

We have derived an approximate theory for the coupled translational and rotational motion of thin hard rods, starting from a microscopic model. The dynamic evolution is determined by binary collisions, in which the normal component of the velocity of the contact point is reversed and the tangential component is either left unchanged (smooth rods) or reversed as well (rough rods). The Mori-Zwanzig projection operator formalism has been applied to the correlation of a tagged rod's density $\rho(\mathbf{r}, \mathbf{u}, t)$, specifying its position \mathbf{r} and orientation \mathbf{u} at a given time t . Matrix elements of the collision operator have been computed, resulting in a generalized Enskog theory, in which only uncorrelated binary collisions are taken into account – similar in spirit to a “Stoßzahl Ansatz” of the corresponding Boltzmann equation. Two steps in a continued fraction expansion give rise to an integral equation for the correlation function. This equation has been solved in the limit of small wavenumber, where it is rendered diagonal by linear combinations of the spherical harmonics. We have also performed numerical simulations, using an event driven algorithm for hard needles.

Purely rotational motion ($\mathbf{k} = 0$) is as expected and in agreement with previous discussions. For small density we observe damped oscillations with a frequency $\omega^2 = T/I$. In the dilute limit it is essential to include free particle motion, which provides the dominant damping mechanism.

For large densities the dynamics is purely relaxational. The crossover happens at a critical density $\rho_{\text{crit}}^2(l) = 8\pi^3 l(l+1)/(c_R W)$ which depends on the angular momentum l , the moment of inertia via $W = \frac{mL^2}{2I}$ and on whether we are considering smooth or rough rods. For $\rho_0 \geq \rho_{\text{crit}}(l)$ our approximate kinetic theory predicts two relaxation times. The longer one is determined by the rotational diffusion constant according to $\tau_{\text{long}}(l) = (D_R l(l+1))^{-1}$ with the rotational diffusion constant D_R given by Eq. (51). It depends on the mass distribution along the rod and is different for smooth and rough needles. The rotational diffusion constant D_R is always larger for smooth rods than for rough rods, e.g. for a homogeneous mass

distribution along the rod we find $D_R^{\text{smooth}}/D_R^{\text{rough}} \approx 1.60$.

The long time relaxation $\tau_{\text{long}}(l) = (D_R l(l+1))^{-1}$ is in agreement with the Perrin equation, where D_R enters as a phenomenological parameter. In addition our theory also predicts a fast decay with a relaxation rate $\tau_{\text{short}} = D_R I/T$ or alternatively $\frac{\tau_{\text{short}}}{\tau_{\text{long}}} = \frac{D_R^2 I}{T} l(l+1) = (\frac{\rho_{\text{crit}}}{2\rho_0})^2$. This short relaxation time is mainly determined by the moment of inertia and hence roughly three times larger for dumbbells than for a homogeneous mass distribution.

Next we discussed purely translational motion ($l = 0$). We find relaxation with a short and a long relaxation time, the latter being diffusive $\tau_l = (D_{\text{iso}} k^2)^{-1}$ and in agreement with the Perrin equation, which allowed us to identify the isotropic diffusion constant D_{iso} as in Eq. (57). It depends on the mass distribution and is different for smooth and rough needles. The isotropic diffusion constant is always larger for smooth needles than for rough ones, e.g. for a homogeneous mass distribution along the rod we find $D_{\text{iso}}^{\text{smooth}}/D_{\text{iso}}^{\text{rough}} \approx 2.36$. Comparing different mass distributions we always find a larger diffusion constant for the homogeneous mass distribution than for the dumbbells. In addition to the diffusive long time decay, the kinetic theory predicts partial decay on a microscopic timescale, which is given by $\tau_0 = D_{\text{iso}} m/T$.

The most interesting case is of course the coupled translational and rotational motion, as described by the time dependent correlation $\Phi_{\mathbf{u},\mathbf{u}'}(\mathbf{k}, t)$. This function has been diagonalised in the long wavelength limit by linear combinations of spherical harmonics, which for general \mathbf{k}, l, m differ from the solution to the Perrin equation. We attribute this difference to the fact that the Perrin equation is *not* simply a gradient expansion but involves the angular momentum operator, which does not contain any small parameter allowing for a systematic expansion.

Anisotropic diffusion is best discussed with the help of the particle's displacement vector, projected onto or perpendicular to the particle's initial orientation, i.e. $\langle \Delta r_{\parallel}^2(t) \rangle$ and $\langle \Delta r_{\perp}^2(t) \rangle$. In general, we find three dynamic regimes. For short times $t \ll \tau_0$ the motion is ballistic. For the longest timescales, i.e. times larger than the timescale for rotation of a needle, $t \gg 1/(6D_R)$, isotropic diffusion prevails. In between a time regime appears which is characterized by anisotropic diffusion: a linear increase of the mean square displacements $\langle \Delta r_{\parallel}^2(t) \rangle \sim D_{\parallel} t$ and $\langle \Delta r_{\perp}^2(t) \rangle \sim D_{\perp} t$ with anisotropic diffusion constants D_{\parallel} and D_{\perp} . To clearly see this intermediate regime, the density has to be sufficiently large, such that the timescale for rotational diffusion of the rods is long. In the simulations these three time

regimes are clearly visible for densities $\rho_0 \geq 40$ (see Fig. 4). The analytical theory correctly predicts anisotropic diffusion qualitatively (see Fig. 4), however for such high densities no quantitative agreement between simulations and theory is achieved, see Fig. 5. Anisotropic diffusion is more pronounced for a higher moment of inertia, the highest value being reached for dumbbells with all the mass concentrated at the endpoints of the needle (see Fig. 6). Lowering the density leads to shrinking of the intermediate time regime, such that for small densities ($\rho_0 \leq 10$) one only observes a crossover from ballistic motion to isotropic diffusion. For these densities the agreement between theory and simulation is very good, as shown in Fig. 3.

Since the intermediate anisotropic regime is only present for high densities, we conclude that the Perrin equation is an adequate description of the dynamics of thin hard rods only for high density. In order to derive it from a microscopic theory, it is not sufficient to let the wavenumber become small; in addition the rotational diffusion constant has to be small or in other words the rotational timescale has to be long.

A perspective for future work based on the microscopic theory presented here would be to exploit the correlation function to calculate intermediate scattering functions. These could then be measured in depolarized light scattering experiments. Moreover, the microscopic theory is valid for all wave vectors. However, up to now, a diagonalization procedure used to derive explicit expressions for $\varphi_{ll'}$ exists only for small wave vectors.

APPENDIX A: MATRIX ELEMENTS

In this appendix, the essential steps necessary to calculate the matrix elements χ_0 , $\Omega_0(\mathbf{u}', \mathbf{u})$, $\chi_1(\mathbf{u}', \mathbf{u})$, and $\Omega_1(\mathbf{u}', \mathbf{u})$ are presented.

1. Generating functional

The structure of the collision operator requires a specific coordinate system for the translational momenta (or velocities).

In fact, the operator $i\mathcal{L}'_+$ appearing in matrix elements is reduced to the N -fold operator

for collision of needle 0 with needle 1,

$$i\mathcal{L}'_+ = N |\mathbf{V} \cdot \mathbf{u}_\perp| \theta(-\mathbf{V} \cdot \mathbf{u}_\perp \sigma) \theta\left(\frac{L}{2} - |s_{01}|\right) \theta\left(\frac{L}{2} - |s_{10}|\right) \delta(|\mathbf{r}_{01}^\perp| - 0^+) (b_{01}^+ - 1). \quad (\text{A1})$$

The equality

$$\frac{d}{dt} |\mathbf{r}_{12}^\perp| = \mathbf{u}_\perp \cdot \mathbf{V}_r \text{sgn}(\mathbf{r}_{12} \cdot \mathbf{u}_\perp) \quad (\text{A2})$$

has been used, and σ is short for $\text{sgn}(\mathbf{r}_{12} \cdot \mathbf{u}_\perp)$. The relative velocity of contact points \mathbf{V} and its representation in the orthonormal basis $\mathbf{u}_\perp, \mathbf{u}_0^\perp, \mathbf{u}_0$ have been defined in section III. Before performing the transformation, let us recall the definition of the integration measure in average $\langle \dots \rangle$ in terms of canonical coordinates:

$$d\Gamma = \prod_{i=0}^1 d\mathbf{r}_i d\varphi_i d\theta_i d\mathbf{p}_{\mathbf{r}_i} dp_{\varphi_i} dp_{\theta_i} \quad (\text{A3})$$

The normalization reads as

$$Z^{-1} = \frac{1}{V^2} \frac{1}{(4\pi)^2} \frac{1}{(2\pi m T)^3} \frac{1}{(2\pi I T)^2} \quad (\text{A4})$$

Next, the canonical coordinates are transformed to new ones which are standard normally distributed (with respect to the Boltzmann factor $\exp(-\beta\mathcal{H})$). Changing moreover translation momenta $\mathbf{p}_{\mathbf{r}_i}$ to CMS momentum and relative momentum, the transformation reads as follows:

$$\boldsymbol{\chi} = \frac{1}{\sqrt{2Tm}} (\mathbf{p}_0 - \mathbf{p}_1) \quad (\text{A5})$$

$$\boldsymbol{\gamma} = \frac{1}{\sqrt{2Tm}} (\mathbf{p}_0 + \mathbf{p}_1) \quad (\text{A6})$$

$$\mathbf{P}_{\theta_i} = \frac{1}{\sqrt{IT}} \mathbf{p}_{\theta_i} \quad (\text{A7})$$

$$\mathbf{P}_{\varphi_i} = \frac{1}{\sqrt{IT}} \frac{\mathbf{p}_{\varphi_i}}{\sin(\theta_i)} \quad (\text{A8})$$

with $i = 0, 1$. Positions are transformed according to

$$\mathbf{r}_{01} = \mathbf{r}_0 - \mathbf{r}_1 \quad (\text{A9})$$

$$\mathbf{r} = \mathbf{r}_0 \quad (\text{A10})$$

The resulting integration with respect to \mathbf{r}_{01} will be split into the following three components:

$$c = \mathbf{r}_{01} \cdot \mathbf{u}_\perp \quad (\text{A11})$$

$$b = s_{10} = \frac{\mathbf{r}_{01} \cdot \mathbf{u}_0^\perp}{\sqrt{1 - (\mathbf{u}_0 \cdot \mathbf{u}_1)^2}} \quad (\text{A12})$$

$$a = -s_{01} = \mathbf{r}_{01} \cdot \mathbf{u}_0 - \frac{(\mathbf{u}_0 \cdot \mathbf{u}_1)(\mathbf{r}_{01} \cdot \mathbf{u}_0^\perp)}{\sqrt{1 - (\mathbf{u}_0 \cdot \mathbf{u}_1)^2}} \quad (\text{A13})$$

This decomposition complements the one for the relative velocity of contact points. The corresponding Jacobian is given by

$$J = \frac{\partial(r_{01}^x, r_{01}^y, r_{01}^z)}{\partial(a, b, c)} = \sqrt{1 - (\mathbf{u}_0 \cdot \mathbf{u}_1)^2} \quad (\text{A14})$$

The relative velocity of contact points given in terms of the new coordinates reads as follows:

$$\begin{aligned} \mathbf{V}_r = \sqrt{\frac{2T}{m}} \boldsymbol{\chi} &- a \sqrt{\frac{T}{I}} (P_{\theta_0} \hat{\mathbf{e}}_{\theta_0} + P_{\varphi_0} \hat{\mathbf{e}}_{\varphi_0}) \\ &- b \sqrt{\frac{T}{I}} (P_{\theta_1} \hat{\mathbf{e}}_{\theta_1} + P_{\varphi_1} \hat{\mathbf{e}}_{\varphi_1}) \end{aligned} \quad (\text{A15})$$

As the velocity \mathbf{V}_r and relative position \mathbf{r}_{01} have been decomposed with respect to the base $(\mathbf{u}_\perp, \mathbf{u}_0^\perp, \mathbf{u}_0)$, the expression given just above will be rewritten likewise. Following a suggestion by Huthmann, one may transform from standard normally distributed variables $(P_{\varphi_i}, P_{\theta_i})$ with respect to the base $(\hat{\mathbf{e}}_{\varphi_i}, \hat{\mathbf{e}}_{\theta_i})$ to new standard normally distributed variables (v_i, w_i) with respect to the base $(\mathbf{u}_i^\perp, \mathbf{u}_\perp)$, giving the following expression for \mathbf{V}_r :

$$\begin{aligned} \mathbf{V}_r = \sqrt{\frac{2T}{m}} \boldsymbol{\chi} &- a \sqrt{\frac{T}{I}} (v_0 \mathbf{u}_0^\perp + w_0 \mathbf{u}_\perp) \\ &- b \sqrt{\frac{T}{I}} (v_1 \mathbf{u}_1^\perp + w_1 \mathbf{u}_\perp) \end{aligned} \quad (\text{A16})$$

Later, on \mathbf{u}_1^\perp will be eliminated using

$$\mathbf{u}_1^\perp = -\tilde{A} \mathbf{u}_0 + \tilde{B} \mathbf{u}_0^\perp \quad (\text{A17})$$

where

$$\tilde{A} = \sqrt{1 - (\mathbf{u}_0 \cdot \mathbf{u}_1)^2} \quad (\text{A18})$$

$$\tilde{B} = (\mathbf{u}_0 \cdot \mathbf{u}_1) \quad (\text{A19})$$

So a decomposition of \mathbf{V}_r with respect to the base $(\mathbf{u}_\perp, \mathbf{u}_0^\perp, \mathbf{u}_0)$ results.

In terms of the variables $(\boldsymbol{\gamma}, \boldsymbol{\chi}, v_0, w_0, v_1, w_1)$ the 2-needle Hamiltonian reads

$$\beta \mathcal{H} = \frac{1}{2} (\boldsymbol{\gamma}^2 + \boldsymbol{\chi}^2 + v_0^2 + w_0^2 + v_1^2 + w_1^2). \quad (\text{A20})$$

Accordingly, the integration measure multiplied by the normalization changes to

$$Z^{-1} d\Gamma = \frac{1}{V^2} \frac{1}{(4\pi)^2} \frac{1}{(2\pi)^5} d\mathbf{r} d\mathbf{a} d\mathbf{b} d\mathbf{c} d\Omega_0 d\Omega_1 d\boldsymbol{\gamma} d\boldsymbol{\chi} dv_0 dw_0 dv_1 dw_1 \quad (\text{A21})$$

where $d\Omega_i = d\varphi_i \sin(\theta_i) d\theta_i$ defines the integration with respect to spatial angles. Now, the collision operator involves a projection of \mathbf{V}_r . Moreover, $\boldsymbol{\gamma}$ is related to \mathbf{V}_r by Eq. (A16). Therefore, $\boldsymbol{\gamma}$ will have to be expressed in terms of \mathbf{V}_r in the integration measure and the Hamiltonian. The integration measure involving a factor by $d\boldsymbol{\chi} = \left(\frac{m}{2T}\right)^{3/2} dx dy dz$, the Hamiltonian is

$$\begin{aligned} \beta\mathcal{H} = \frac{1}{2} & \left[\frac{m}{2T}(x^2 + y^2 + z^2) + (v_0^2 + w_0^2) \left(1 + a^2 \frac{m}{2I}\right) \right. \\ & + (v_1^2 + w_1^2) \left(1 + b^2 \frac{m}{2I}\right) + x \frac{m}{T} \sqrt{\frac{T}{I}} (aw_0 + bw_1) \\ & + y \frac{m}{T} \sqrt{\frac{T}{I}} (\tilde{B}bv_1 + av_0) - z \frac{m}{T} \sqrt{\frac{T}{I}} (\tilde{A}bv_1) \\ & \left. + ab \frac{m}{I} \tilde{B}v_0v_1 + ab \frac{m}{I} w_0w_1 + \boldsymbol{\gamma}^2 \right] \end{aligned} \quad (\text{A22})$$

The variable x will require a particular treatment as will be shown later on. Moreover, the variable $\boldsymbol{\gamma}$, denoting the CMS momentum, will not appear in matrix elements involving only relative translational momenta, and therefore will be treated separately. Defining the vector \mathbf{X} by

$$\mathbf{X}^T = (y, z, v_0, w_0, v_1, w_1) \quad (\text{A23})$$

the Hamiltonian may be rewritten in the following form

$$\beta\mathcal{H} = \frac{1}{2} \mathbf{X}^T \mathbf{A} \mathbf{X} + \frac{1}{2} \left(\frac{m}{2T} x^2 + x \frac{m}{T} \sqrt{\frac{T}{I}} (aw_0 + bw_1) \right) + \frac{1}{2} \boldsymbol{\gamma}^2 \quad (\text{A24})$$

where \mathbf{A} is the following matrix:

$$\mathbf{A} = \begin{pmatrix} \frac{m}{2T} & 0 & \frac{m}{2T} \sqrt{\frac{T}{I}} a & 0 & \frac{m}{2T} \sqrt{\frac{T}{I}} b \tilde{B} & 0 \\ 0 & \frac{m}{2T} & 0 & 0 & \frac{m}{2T} \sqrt{\frac{T}{I}} \tilde{A} b & 0 \\ \frac{m}{2T} \sqrt{\frac{T}{I}} a & 0 & (1 + a^2 \frac{m}{2I}) & 0 & ab \frac{m}{2I} \tilde{B} & 0 \\ 0 & 0 & 0 & (1 + a^2 \frac{m}{2I}) & 0 & ab \frac{m}{2I} \\ \frac{m}{2T} \sqrt{\frac{T}{I}} b \tilde{B} & \frac{m}{2T} \sqrt{\frac{T}{I}} \tilde{A} b & ab \frac{m}{2I} \tilde{B} & 0 & (1 + b^2 \frac{m}{2I}) & 0 \\ 0 & 0 & 0 & ab \frac{m}{2I} & 0 & (1 + b^2 \frac{m}{2I}) \end{pmatrix} \quad (\text{A25})$$

Let us now consider the generating functional with respect to

$$\mathbf{H}^T = (h_y, h_z, h_{v_0}, h_{w_0}, h_{v_1}, h_{w_1}), \quad (\text{A26})$$

namely

$$\begin{aligned}
G(\mathbf{H}) &= \int d\mathbf{X} \exp(-\beta\mathcal{H} + \mathbf{H}^T \mathbf{X}) \\
&= \int d\mathbf{X} \exp\left(-\frac{1}{2}\mathbf{X}^T \mathbf{A} \mathbf{X} - \frac{1}{2}\left(\frac{m}{2T}x^2 + x\frac{m}{T}\sqrt{\frac{T}{I}}(aw_0 + bw_1)\right) + \mathbf{H}^T \mathbf{X}\right)
\end{aligned} \tag{A27}$$

The integration is gaussian and the result is:

$$G(\mathbf{H}) = (2\pi)^3 \frac{2T}{m} \left(1 + \frac{m}{2I}(a^2 + b^2)\right)^{-1/2} \exp(-\beta\mathcal{H}_{\text{eff}}) \tag{A28}$$

with the effective Hamiltonian

$$\begin{aligned}
\beta\mathcal{H}_{\text{eff}} &= \frac{x^2}{2} \left(\frac{m}{2T}\right) \frac{1}{\left(1 + \frac{m}{2I}(a^2 + b^2)\right)} - \frac{1}{2}\mathbf{H}^T \mathbf{A}^{-1} \mathbf{H} + \frac{1}{2}\gamma^2 \\
&+ x \frac{m}{2T \left(1 + \frac{m}{2I}(a^2 + b^2)\right)} \sqrt{\frac{T}{I}} (ah_{w_0} + bh_{w_1})
\end{aligned} \tag{A29}$$

The inverse matrix \mathbf{A}^{-1} is given by

$$\begin{pmatrix}
\frac{2T}{m} \left(1 + \frac{m}{2I}(a^2 + b^2\tilde{B}^2)\right) & -\frac{T}{I}(\tilde{A}\tilde{B}b^2) & -\sqrt{\frac{T}{I}}a & 0 & -\sqrt{\frac{T}{I}}b\tilde{B} & 0 \\
-\frac{T}{I}(\tilde{A}\tilde{B}b^2) & \frac{2T}{m} \left(1 + \frac{m}{2I}b^2\tilde{A}^2\right) & 0 & 0 & \sqrt{\frac{T}{I}}\tilde{A}b & 0 \\
-\sqrt{\frac{T}{I}}a & 0 & 1 & 0 & 0 & 0 \\
0 & 0 & 0 & \frac{1+b^2\frac{m}{2I}}{1+\frac{m}{2I}(a^2+b^2)} & 0 & -\frac{ab\frac{m}{2I}}{1+\frac{m}{2I}(a^2+b^2)} \\
-\sqrt{\frac{T}{I}}b\tilde{B} & \sqrt{\frac{T}{I}}\tilde{A}b & 0 & 0 & 1 & 0 \\
0 & 0 & 0 & -\frac{ab\frac{m}{2I}}{1+\frac{m}{2I}(a^2+b^2)} & 0 & \frac{1+a^2\frac{m}{2I}}{1+\frac{m}{2I}(a^2+b^2)}
\end{pmatrix} \tag{A30}$$

Whenever matrix elements involving the collision operator appear, the delta function $\delta(|\mathbf{r}_{01}^\perp| - 0^+) = \delta(|c| - 0^+)$ in terms of new position coordinates as well as the dependance on $\text{sgn}(c)$ need to be taken care of. In this case the following relation is useful:

$$\begin{aligned}
\int_{-\infty}^{\infty} dc \delta(|c| - 0^+) \dots f(\dots, \text{sgn}(c)) &= \lim_{\epsilon \rightarrow 0^+} \int_{-\infty}^{\infty} dc (\delta(c + \epsilon) + \delta(c - \epsilon)) \dots f(\dots, \text{sgn}(c)) \\
&= \dots (f(\dots, +1) + f(\dots, -1))
\end{aligned} \tag{A31}$$

2. Matrix elements

Matrix elements explicitly involving the collision operator can be easily calculated when represented as moments of the variables $(x, y, z, v_0, w_0, v_1, w_1, \gamma)$ using the generating functional derived above. In fact moments involving $(y, z, v_0, w_0, v_1, w_1)$ can be obtained by replacing expression involving a variable say y to some power by the respective derivative with the order equaling the power. The integrations with respect to x and γ are treated separately.

In fact, a matrix element $\langle A^* i\mathcal{L}'_+ A \rangle$ usually has the following form

$$\begin{aligned} \langle A^* i\mathcal{L} A \rangle &= C \int_{-L/2}^{L/2} da \int_{-L/2}^{L/2} db \\ &\times \int \dots \int_{\Omega_0, \Omega_1, x, y, z, v_0, w_0, v_1, w_1, \gamma} J(\Omega_0, \Omega_1) e^{-\beta \mathcal{H}} \\ &\times (\Theta(-x) + \Theta(x)) |x| \\ &\times f(\Omega_0, \Omega_1, x, y, z, v_0, w_0, v_1, w_1, \gamma) \end{aligned} \quad (\text{A32})$$

where

$$C = \frac{1}{Z} V N(m/2T)^{3/2} \quad (\text{A33})$$

The function $f(\Omega_0, \Omega_1, x, y, z, v_0, w_0, v_1, w_1, \gamma)$ contains the functional form of the factors A^* and A in the matrix element after $(b_{01}^+ - 1)$ has been carried out. Other factors arising from the collision operator have been written separately. The factor C is a normalization factor which results after integrating with respect to the CMS position \mathbf{r} and transforming from χ to (x, y, z) . The generating functional now permits reducing the number of integrations as follows:

$$\begin{aligned} \langle A^* i\mathcal{L} A \rangle &= C \int_{-L/2}^{L/2} da \int_{-L/2}^{L/2} db \int \dots \int_{\Omega_0, \Omega_1, x, \gamma} J(\Omega_0, \Omega_1) (\Theta(-x) + \Theta(x)) |x| \\ &\times f(\Omega_0, \Omega_1, x, \gamma, \partial_{h_y}, \partial_{h_z}, \partial_{h_{v_0}}, \partial_{h_{w_0}}, \partial_{h_{v_1}}, \partial_{h_{w_1}}) G(\mathbf{H}) \end{aligned} \quad (\text{A34})$$

In our case, no dependences on γ exist, so the corresponding integration may be immediately carried out, giving a factor of $(2\pi)^{3/2}$.

Let us outline the calculation for the matrix element $\Omega_1(\mathbf{u}', \mathbf{u})$. It involves 2 matrix elements $\langle B_i^* \mathcal{L} B_i \rangle$ for $i = 1, 2$ resulting from the two terms in $\dot{A}_{\mathbf{u}}$. Taking into account the

change of $\Delta \mathbf{u}_0$ and $\Delta \mathbf{p}$ after a collision (which are given for the general case by Eq.s(18) and (24)), the matrix element reads as follows:

$$\begin{aligned} \langle B_1^* \mathcal{L} B_1 \rangle &= (-i) C \int_{-L/2}^{L/2} da \int_{-L/2}^{L/2} db \int \dots \int_{\Omega_0, \Omega_1, x, y, z, v_0, w_0, v_1, w_1} J \\ &\times e^{-\beta \mathcal{H}} \left(\mathbf{k} \cdot \frac{1}{2} \left(\mathbf{V}_r + a \sqrt{\frac{T}{I}} (v_0 \mathbf{u}_0^\perp + w_0 \mathbf{u}_\perp) + b \sqrt{\frac{T}{I}} (v_1 \mathbf{u}_1^\perp + w_1 \mathbf{u}_\perp) \right) \right) \\ &\times |x| (\theta(-x) + \theta(x)) \frac{1}{m} \mathbf{k} \cdot (\alpha \mathbf{u}_\perp + \gamma_1 \mathbf{u}_0 + \gamma_2 \mathbf{u}_0^\perp) \delta(\mathbf{u}' - \mathbf{u}_0) \delta(\mathbf{u} - \mathbf{u}_0) \end{aligned} \quad (\text{A35})$$

and

$$\begin{aligned} \langle B_2^* \mathcal{L} B_2 \rangle &= (-i) \nabla_{\mathbf{u}'}^\mu \nabla_{\mathbf{u}}^\nu C \int_{-L/2}^{L/2} da \int_{-L/2}^{L/2} db \int \dots \int_{\Omega_0, \Omega_1, x, y, z, v_0, w_0, v_1, w_1} J \\ &\times \frac{am}{2I} e^{-\beta \mathcal{H}} \left(\mathbf{u}_0 (\mathbf{u}_0 \cdot \mathbf{V}_r) + \mathbf{u}_0 (\mathbf{u}_0 \cdot \mathbf{u}_1^\perp) b \sqrt{\frac{T}{I}} v_1 - \mathbf{V}_r - a \sqrt{\frac{T}{I}} (v_0 \mathbf{u}_0^\perp + w_0 \mathbf{u}_\perp) - b \sqrt{\frac{T}{I}} (v_1 \mathbf{u}_1^\perp + w_1 \mathbf{u}_\perp) \right) \\ &\times |x| (\theta(-x) + \theta(x)) \left(-\frac{a}{I} \right) (\alpha \mathbf{u}_\perp + \gamma_2 \mathbf{u}_0^\perp)_\nu \delta(\mathbf{u}' - \mathbf{u}_0) \delta(\mathbf{u} - \mathbf{u}_0) \end{aligned} \quad (\text{A36})$$

The coefficients α , γ_1 , and γ_2 are defined in Eq.s (17) and (19), and contain dependancies on x , y , z , $(\mathbf{u}_0 \cdot \mathbf{u}_1)$, as well as a and b .

Using the generating functional as above one finds the following results,

$$\langle B_1^* \mathcal{L} B_1 \rangle = i n_0 \frac{1}{8\pi^{5/2}} \left(\frac{T}{m} \right)^{3/2} L^2 [c_\parallel (\mathbf{k} \cdot \mathbf{u})^2 + c_\perp (k^2 - (\mathbf{k} \cdot \mathbf{u})^2)] \delta(\mathbf{u}' - \mathbf{u}) \quad (\text{A37})$$

$$\langle B_2^* \mathcal{L} B_2 \rangle = i n_0 \frac{1}{8\pi^{5/2}} \left(\frac{T}{m} \right)^{3/2} L^4 \left(\frac{m^2}{I^2} \right) c_R \hat{L}^2 \delta(\mathbf{u}' - \mathbf{u}) \quad (\text{A38})$$

The coefficients c_\parallel , c_\perp , and c_R contain the remaining integrations over a , b , and the relative angle between Ω_0 and Ω_1 , and are defined in appendix B. Adding the two matrix elements gives the expression for $\Omega_1(\mathbf{u}', \mathbf{u})$ in Eq. (38).

APPENDIX B: SOME GEOMETRICAL INTEGRALS

Let us first define

$$I_i = \int_{-1/2}^{1/2} da \int_{-1/2}^{1/2} db \frac{a^i}{\sqrt{1 + W(a^2 + b^2)}} \quad (\text{B1})$$

The constants appearing in Eq.(38) are given explicitly as follows where $W = mL^2/(2I)$

$$c_{\parallel} = \left(\frac{1+\beta}{2}\right) 2\pi \int_{-1/2}^{1/2} da \int_{-1/2}^{1/2} db (1+W(a^2+b^2))^{1/2} \\ \times \int_{-1}^1 dx (1-x^2)^{1/2} \frac{(1+Wa^2+Wb^2x^2)}{(1+W(a^2+b^2)+W^2a^2b^2(1-x^2))} \quad (\text{B2})$$

$$c_{\perp} = \pi^2 I_0 + \left(\frac{1+\beta}{2}\right) \pi \int_{-1/2}^{1/2} da \int_{-1/2}^{1/2} db (1+W(a^2+b^2))^{1/2} \\ \times \int_{-1}^1 dx (1-x^2)^{1/2} \frac{(1+Wb^2(1-x^2))}{(1+W(a^2+b^2)+W^2a^2b^2(1-x^2))} \quad (\text{B3})$$

$$c_R = \pi^2 I_2 + \left(\frac{1+\beta}{2}\right) \pi \int_{-1/2}^{1/2} da \int_{-1/2}^{1/2} db a^2 (1+W(a^2+b^2))^{1/2} \\ \times \int_{-1}^1 dx (1-x^2)^{1/2} \frac{(1+Wb^2(1-x^2))}{(1+W(a^2+b^2)+W^2a^2b^2(1-x^2))} \quad (\text{B4})$$

They have been evaluated numerically for $W = 6$ and $W = 2$ (see Table I).

APPENDIX C: SOME PROPERTIES OF SPHEROIDAL WAVE FUNCTIONS

For a general introduction to spheroidal wave functions we refer the reader to Refs. 29,30. In this work we only need spheroidal functions of either prolate or oblate type. The prolate functions are defined as the solutions of the eigenvalue equation

$$\left(\frac{d}{d\eta}(1-\eta^2)\frac{d}{d\eta} + \lambda_{lm}(\zeta) - \frac{m^2}{1-\eta^2} - \zeta^2\eta^2\right) S_{lm}(\zeta, \eta) = 0, \quad (\text{C1})$$

where $l \geq 0$ and m are integers obeying $-l \leq m \leq l$ and ζ is a real constant. The oblate functions can be obtained from $S_{lm}(\zeta, \eta)$ by replacing ζ by $i\zeta$. We prefer working with an orthonormal basis and therefore choose the normalization

$$\int d\eta S_{lm}^*(\zeta, \eta) S_{l'm}(\zeta, \eta) = \delta_{ll'} \quad (\text{C2})$$

which is unfortunately different from the one used in Refs. 29,30.

The $S_{lm}(\zeta, \eta)$ can be expressed in terms of associated Legendre functions P_{lm} as

$$S_{lm}(\zeta, \eta) = \frac{1}{N_{lm}(\zeta)} \sum_r' d_r^{lm}(\zeta) P_{r+m,m}(\eta). \quad (\text{C3})$$

Here $d_r^{lm}(\zeta)$ are expansion coefficients and

$$N_{lm}(\zeta) = \sqrt{\sum_r' (d_r^{lm}(\zeta))^2 \frac{2}{2r+2m+1} \frac{(r+2m)!}{r!}} \quad (\text{C4})$$

is the normalization constant. For methods to obtain $\lambda_{lm}(\zeta)$ and d_r^{lm} from Eq. (C1) we again refer the reader to Refs. 29,30. For our purposes it is sufficient to know the eigenvalues $\lambda_{lm}(\zeta)$ up to order ζ^2 and the scalar product

$$(S_{lm}(\zeta), S_{l'm}(0)) \equiv \int d\eta S_{lm}^*(\zeta, \eta) S_{l'm}(0, \eta) \quad (C5)$$

up to order ζ^4 . The results of this tedious calculation (which is omitted here for the sake of brevity) are

$$\lambda_{lm}(\zeta) = \lambda_{lm}^{(0)} + \zeta^2 \lambda_{lm}^{(2)} + \mathcal{O}(\zeta^4) \quad (C6)$$

$$= l(l+1) + \zeta^2 \frac{2l(l+1) - 2m^2 - 1}{(2l+3)(2l-1)} + \mathcal{O}(\zeta^4) \quad (C7)$$

and

$$(S_{lm}(\zeta), S_{l'm}(0)) = \delta_{ll'} + \zeta^2 g_{ml'l'} + \zeta^4 h_{ml'l'} + \mathcal{O}(\zeta^6) \quad (C8)$$

where

$$g_{ml'l'} = \delta_{l,l'+2} \frac{\sqrt{(l-1-m)(l-1+m)(l-m)(l+m)}}{2(2l-1)^2 \sqrt{(2l-3)(2l+1)}} - \delta_{l+2,l'} \frac{\sqrt{(l'-1-m)(l'-1+m)(l'-m)(l'+m)}}{2(2l'-1)^2 \sqrt{(2l'-3)(2l'+1)}} \quad (C9)$$

$$h_{ml'l'} = \frac{1 - \delta_{ll'}}{\lambda_{lm}^{(0)} - \lambda_{l'm}^{(0)}} (a_{l'm} g_{ml,l'-2} + a_{l'+2,m} g_{ml,l'+2}) - \frac{\lambda_{lm}^{(2)} - \lambda_{l'm}^{(2)}}{\lambda_{lm}^{(0)} - \lambda_{l'm}^{(0)}} g_{ml'l'} - \frac{1}{2} \delta_{ll'} (g_{ml,l+2}^2 + g_{ml,l-2}^2) \quad \text{and} \quad (C10)$$

$$a_{lm} = \frac{\sqrt{(l-1+m)(l-1-m)(l+m)(l-m)}}{(2l-1)\sqrt{(2l+1)(2l-3)}}. \quad (C11)$$

Here it is implied that all coefficients are 0 if their indices lie outside their range of validity $l, l' \geq 0$ and $-l, -l' \leq m \leq l, l'$. For some values of the indices the coefficients appear to have vanishing denominators. However, in these cases the prefactors are 0, too, and the respective terms should be taken to be 0.

APPENDIX D: DIAGONALIZATION OF Φ

In order to diagonalize the matrix of correlation functions $\varphi_{\eta\eta'}(\mathbf{k}, z)$, it is sufficient to diagonalize $B_{\eta\eta'} = z(\chi^{-1})_{\eta\eta'} + (\chi^{-1}\Omega\chi^{-1})_{\eta\eta'}$. Since $\chi_{\eta\eta'}$ is diagonal in the basis of (normalized)

Legendre polynomials $\sqrt{l + \frac{1}{2}}P_l(\eta) = S_{l0}(0, \eta)$ and $\Omega_{\eta\eta'}$ is diagonal in the basis of $S_{l0}(ic, \eta)$, where $c^2 = (c_\perp - c_\parallel)L^2k^2/(4W^2c_R)$ is small in the limit $k^2 \rightarrow 0$, we aim at a perturbative solution. The starting point is the representation of B in the basis $\{S_{l0}(0, \eta)\}$. The matrix elements are

$$B_{ll'} = \int d\eta d\eta' S_{l0}(0, \eta) B_{\eta\eta'} S_{l'0}(0, \eta'). \quad (\text{D1})$$

Since χ is already diagonal in this basis, nothing needs to be done for the term $z\chi^{-1}$ and we get $z(\chi^{-1})_{ll'} = z\delta_{ll'}/\chi_l$.

The term $\chi^{-1}\Omega\chi^{-1}$ is more complicated. Inserting $\mathbf{1} = \sum_l |S_{l0}(ic)\rangle\langle S_{l0}(ic)|$ in the two places between χ^{-1} and Ω we get

$$B_{ll'} = z\delta_{ll'}/\chi_l + (\chi^{-1}\Omega\chi^{-1})_{ll'} \quad (\text{D2})$$

$$= z\delta_{ll'}/\chi_l + \delta_{ll'} \frac{\Omega_l}{\chi_l^2} + \Delta B_{ll'}^1 + \Delta B_{ll'}^2 + \Delta B_{ll'}^3, \quad \text{where} \quad (\text{D3})$$

$$\Delta B_{ll'}^1 = c^2 g_{0ll'} \frac{\Omega_l - \Omega_{l'}}{\chi_l \chi_{l'}}, \quad (\text{D4})$$

$$\Delta B_{ll'}^2 = \frac{c^4}{\chi_0} (h_{0l'0} \frac{\Omega_{l'}}{\chi_{l'}} \delta_{l0} + h_{0l0} \frac{\Omega_l}{\chi_l} \delta_{l'0}), \quad (\text{D5})$$

$$\Delta B_{ll'}^3 = \frac{c^4}{\chi_l \chi_{l'}} \sum_j g_{0jl} g_{0jl'} \Omega_j \quad (\text{D6})$$

to order k^2 . The calculation is straightforward but care has to be taken with χ_0 and Ω_0 as they are of order k^2 while all other eigenvalues of χ and Ω are of order 1. Therefore the matrix elements ΔB_{02}^1 and ΔB_{20}^1 are of order 1. However, all other off-diagonal matrix elements of B are of order k^2 or smaller. The diagonal element B_{00} is of order $1/k^2$ while all other diagonal elements are of order 1. In order to be able to use perturbation theory we employ a Jacobi transformation

$$R_{ll'} = \delta_{ll'} + (\cos \frac{B_{02}}{B_{00}} - 1)(\delta_{l0}\delta_{l'0} + \delta_{l2}\delta_{l'2}) + \sin \frac{B_{02}}{B_{00}}(\delta_{l0}\delta_{l'2} - \delta_{l2}\delta_{l'0}). \quad (\text{D7})$$

which makes $RBR^T = D + k^2\Delta$ where D is a diagonal matrix and Δ is a perturbation. Note that R is really only required up to order k^2 which is

$$R_{ll'} = \delta_{ll'} + \frac{B_{02}}{B_{00}}(\delta_{l0}\delta_{l'2} - \delta_{l2}\delta_{l'0}) + \mathcal{O}(k^4). \quad (\text{D8})$$

The eigenvalues b_l of B (up to order k^2) are given by the diagonal entries of RBR^T since the Jacobi transformation merely changes the basis vectors but not the eigenvalues. The

diagonal entries of RBR^T are equal to $b_l = B_{ll} = z/\chi_l + \Omega_l/\chi_l^2$ for all $l \neq 0, 2$. For the two exceptions one gets $b_0 = B_{00} + 2B_{02}^2/B_{00}$ ($l = 0$) and $b_2 = B_{22} - B_{02}^2/B_{00}$ ($l = 2$). These are, however, higher order corrections which are irrelevant for our purposes and we may therefore use $b_l = z/\chi_l + \Omega_l/\chi_l^2$ for all l .

Finally, the eigenfunctions $S'_l(\eta)$ can be obtained through perturbation theory. The matrix $B_{ll'}$ is symmetric but not normal (i.e. $[B, B^\dagger] \neq 0$, except if z happens to be purely imaginary). Therefore B and of course also RBR^T do not have an orthogonal system of eigenvectors and we have to calculate both left and right eigenvectors perturbatively. This procedure yields for the matrix O^r of right eigenvectors of RBR^T ($O_{ll'}^r$ is the l' th component of the l th eigenvector),

$$O_{ll'}^r = \delta_{ll'} + (1 - \delta_{ll'}) \frac{(RBR^T)_{ll'}}{b_l - b_{l'}}, \quad (\text{D9})$$

while the matrix O^l of left eigenvectors is

$$O_{ll'}^l = \delta_{ll'} + (1 - \delta_{ll'}) \frac{(RBR^T)_{ll'}^*}{(b_l - b_{l'})^*} = (O_{ll'}^r)^* \quad (\text{D10})$$

and the asterisk denotes the complex conjugate.

The right and left eigenfunctions $S_l^r(\eta)$ and $S_l^l(\eta)$ of the original operator B are then

$$S_l^r(\eta) = \sum_{l'} (O^{r*} R)_{ll'} S_{l'0}(0, \eta) \quad (\text{D11})$$

$$S_l^l(\eta) = \sum_{l'} (O^l R)_{ll'}^* S_{l'0}(0, \eta). \quad (\text{D12})$$

The product $O^l R$ is, up to order k^2 ,

$$(O^l R)_{ll'} = \delta_{ll'} + \frac{B_{02}}{B_{00}} (\delta_{l0} \delta_{l'2} - \delta_{l2} \delta_{l'0}) + \quad (\text{D13})$$

$$(1 - \delta_{ll'}) \frac{(RBR^T)_{ll'}^*}{(b_l - b_{l'})^*} \quad (\text{D14})$$

As an application which is needed in the main text we calculate some matrix elements of the correlation function φ in the basis of spherical functions $S_{l0}(0, \eta)$. We have

$$\varphi_{ll'} = - \sum_m (S_{l0}(0) | S_m^r) \frac{1}{z - \frac{4\pi}{b_m}} (S_m^l | S_{l'0}(0)) \quad (\text{D15})$$

$$= - \sum_m (O^{r*} R)_{ml} \frac{1}{z - \frac{4\pi}{b_m}} (O^l R)_{ml'}, \quad (\text{D16})$$

and from this and Eq. (D14) we get

$$\varphi_{00} = -\frac{1}{z - \frac{4\pi}{b_0}} = -\frac{z + \Omega_0/\chi_0}{z(z + \Omega_0/\chi_0) - 4\pi\chi_0}, \quad (\text{D17})$$

omitting terms of higher order than k^2 . Likewise we obtain

$$\varphi_{20} = -\frac{B_{02}}{B_{00}} \frac{1}{z - \frac{4\pi}{b_0}} + \frac{B_{02}}{B_{00}} \frac{1}{z - \frac{4\pi}{b_2}} \quad (\text{D18})$$

$$= 4\pi \frac{c^2}{9\sqrt{5}} \frac{-\Omega_2}{(z^2 + z\chi_0^{-1}\Omega_0 - 4\pi\chi_0)(z^2 + z\chi_2^{-1}\Omega_2 - 4\pi\chi_2)}. \quad (\text{D19})$$

-
- ¹ P. Debye, *Polar molecules* (Dover, New York, 1929).
 - ² F. Perrin, J. de Phys. et le Rad. **5**, 497 (1934).
 - ³ F. Perrin, J. de Phys. et le Rad. **7**, 1 (1936).
 - ⁴ B. J. Berne and R. Pecora, *Dynamic Light Scattering* (John Wiley & Sons, New York, 1976).
 - ⁵ J. Riseman and J. Kirkwood, J. Chem. Phys. **18**, 512 (1950).
 - ⁶ S. Broersma, J. Chem. Phys. **32**, 1626 (1960).
 - ⁷ T. Yoshizaki and H. Yamakawa, J. Chem. Phys. **72**, 57 (1980).
 - ⁸ T. Schilling and D. Frenkel, Phys. Rev. Lett. **92**, 085505 (2004).
 - ⁹ M. M. Tirado and J. G. de la Torre, J. Chem. Phys. **71**, 2581 (1979).
 - ¹⁰ M. M. Tirado, C. L. Martínez, and J. G. de la Torre, J. Chem. Phys. **81**, 2047 (1984).
 - ¹¹ W. Eimer and R. Pecora, J. Chem. Phys. **94**, 2324 (1991).
 - ¹² R. G. Cole, D. K. Hoffman, and G. T. Evans, J. Chem. Phys. **80**, 5365 (1984).
 - ¹³ R. G. Cole, D. R. Evans, and D. K. Hoffman, J. Chem. Phys. **82**, 2061 (1985).
 - ¹⁴ R. G. Cole and G. T. Evans, Ann. Rev. Phys. Chem. **37**, 105 (1986).
 - ¹⁵ G. T. Evans, J. Chem. Phys. **88**, 5035 (1988).
 - ¹⁶ S. R. Aragon and R. Pecora, J. Chem. Phys. **66**, 2506 (1977).
 - ¹⁷ S. R. Aragon, J. Chem. Phys. **73**, 1576 (1980).
 - ¹⁸ S. R. Aragon and R. Pecora, J. Chem. Phys. **82**, 5346 (1985).
 - ¹⁹ K. M. Zero and R. Pecora, Macromolecules **15**, 87 (1982).
 - ²⁰ D. Lehner, H. Lindner, and O. Glatter, Langmuir **16**, 1689 (2000).
 - ²¹ R. Cush, D. Dorman, and P. S. Russo, Macromolecules **37**, 9577 (2004).

- ²² P. S. Russo, in *Dynamic light scattering*, edited by W. Brown (Clarendon Press, Oxford, 1993).
- ²³ D. Frenkel and J. F. Maguire, *Mol. Phys.* **49**, 503 (1983).
- ²⁴ J. J. Magda, H. T. Davis, and M. Tirrell, *J. Chem. Phys.* **85**, 6674 (1986).
- ²⁵ M. Doi and S. F. Edwards, *The theory of polymer dynamics* (Clarendon Press, Oxford, 1986).
- ²⁶ G. Szamel, *Phys. Rev. Lett.* **70**, 3744 (1993).
- ²⁷ G. Szamel and K. Schweizer, *J. Chem. Phys.* **100**, 3127 (1994).
- ²⁸ S. Chapman and T. G. Cowling, *The mathematical theory of nonuniform gases* (Plenum Press, New York, 1960).
- ²⁹ C. Flammer, *Spheroidal wave functions* (Stanford University, Stanford, 1957).
- ³⁰ J. A. Stratton, P. M. Morse, L. J. Chu, J. D. C. Little, and F. J. Corbató, *Spheroidal wave functions* (John Wiley & Sons, New York, 1956).
- ³¹ B. Cichocki, *Z. Phys. B* **66**, 537 (1987).
- ³² T. Aspelmeier, M. Huthmann, and A. Zippelius, in *Lecture Notes in Physics*, edited by T. Pöschel and S. Luding (Springer-Verlag, Berlin, 2001), vol. 564, pp. 31–58.
- ³³ D. K. Hoffman, *J. Chem. Phys.* **50**, 4823 (1969).
- ³⁴ J. D. Verlin, M. K. Matzen, and D. K. Hoffman, *J. Chem. Phys.* **62**, 4146 (1975).
- ³⁵ M. Huthmann, T. Aspelmeier, and A. Zippelius, *Phys. Rev. E* **60**, 654 (1999).
- ³⁶ M. Abramowitz and I. A. Stegun, *Handbook of mathematical functions* (Dover Publications, New York, 1965).

FIG. 1: The collision plane E_{01} spanned by the orientations of two rods.

FIG. 2: Orientational correlation function $\varphi_{11}(\omega)$ from theory (Eq. (55)) and simulation for various densities ρ_0 .

FIG. 3: Mean square displacements r_{\parallel}^2 and r_{\perp}^2 for homogeneous rods ($W = 6$) at densities $\rho_0 = 4$ and $\rho_0 = 10$ from theory and simulations. The uppermost line indicates the exact ballistic behavior for small times. Distances are measured in dimensionless units with $L = 1$.

FIG. 4: Mean square displacements r_{\parallel}^2 and r_{\perp}^2 for homogeneous rods ($W = 6$) at densities $\rho_0 = 40$ (simulation) and $\rho_0 = 100$ (theory). At these densities, an anisotropy window opens up between the parallel and perpendicular mean-square displacements.

FIG. 5: Mean square displacements r_{\parallel}^2 and r_{\perp}^2 for homogeneous rods ($W = 6$) at densities $\rho_0 = 40$ and $\rho_0 = 100$.

FIG. 6: Mean square displacements for dumbbell molecules with $W = 2$.

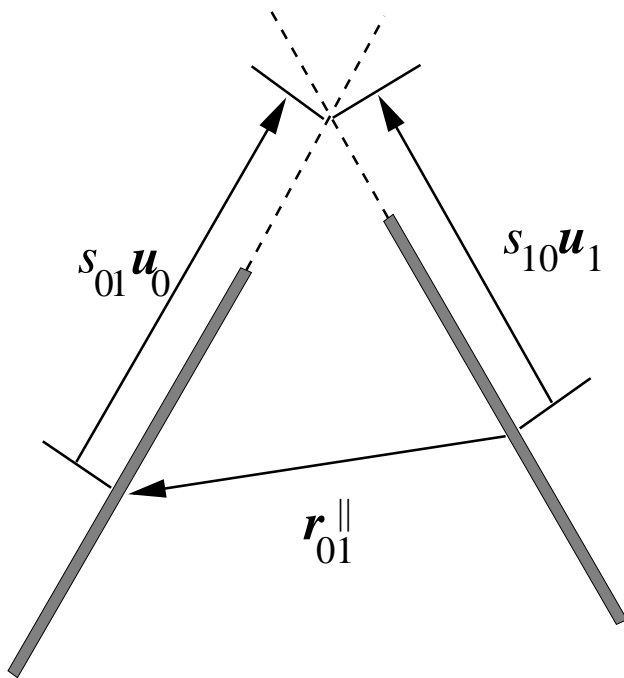


FIG. 1

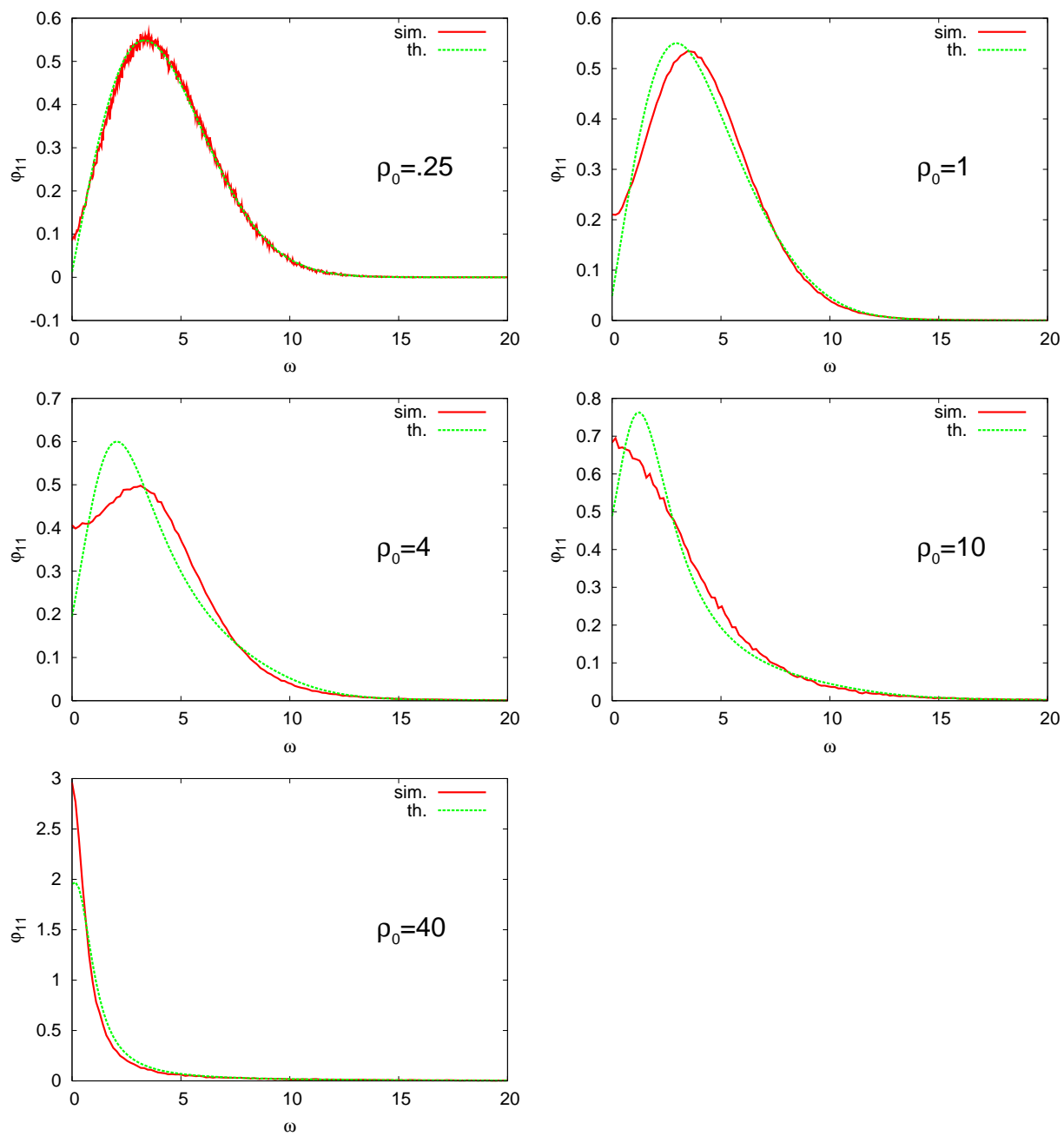


FIG. 2

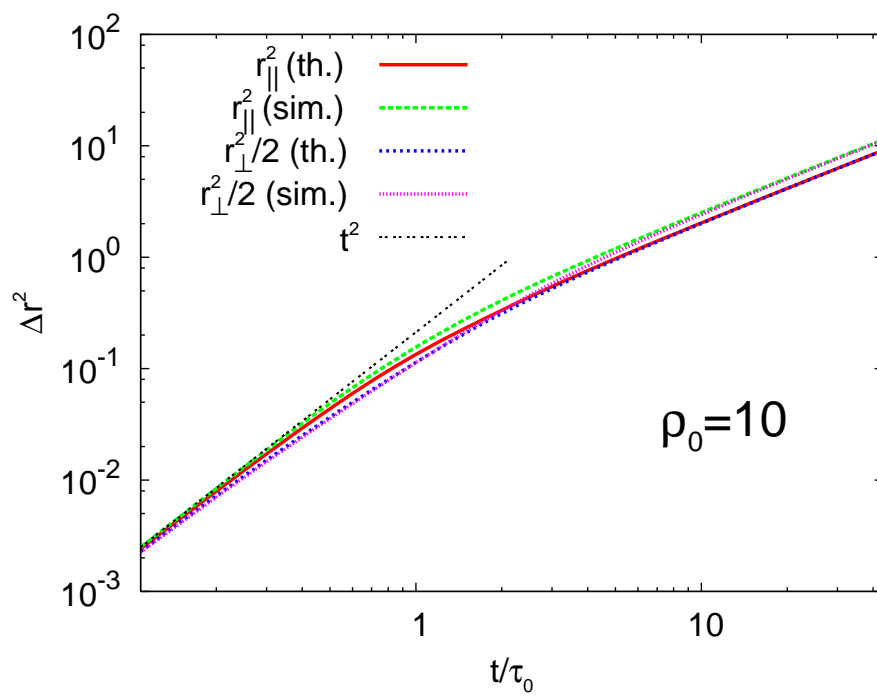
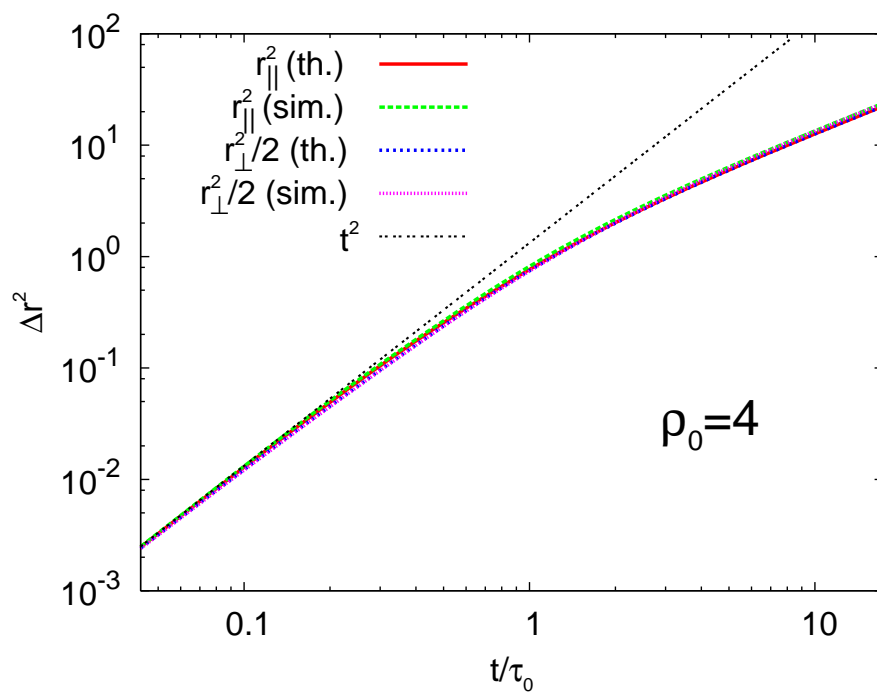


FIG. 3

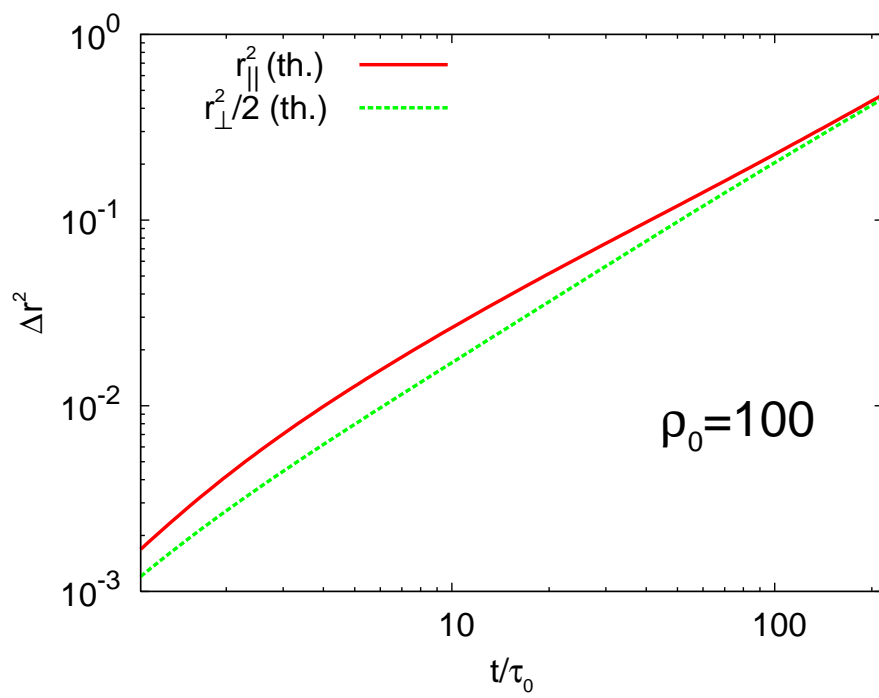
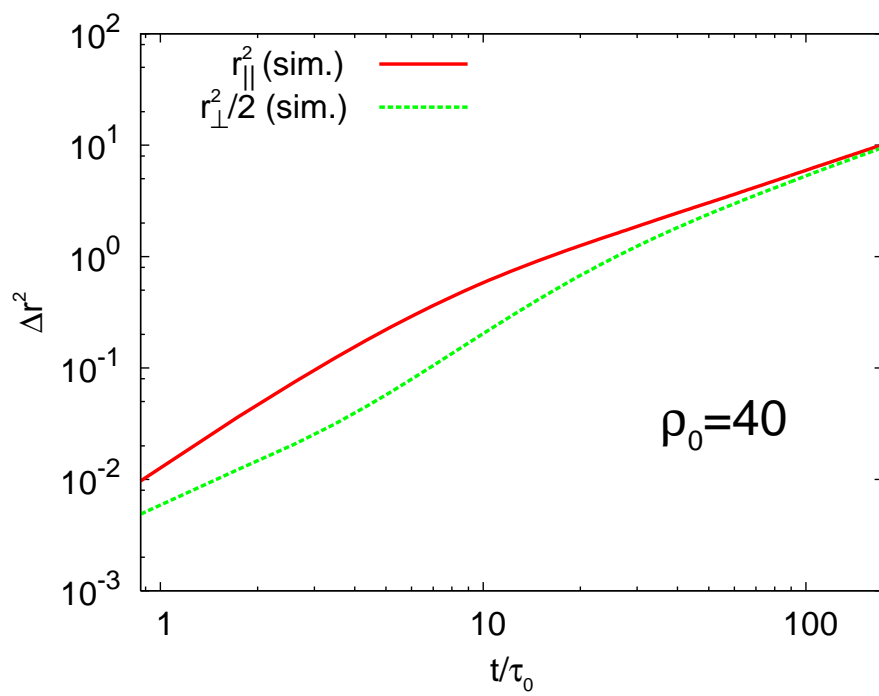


FIG. 4

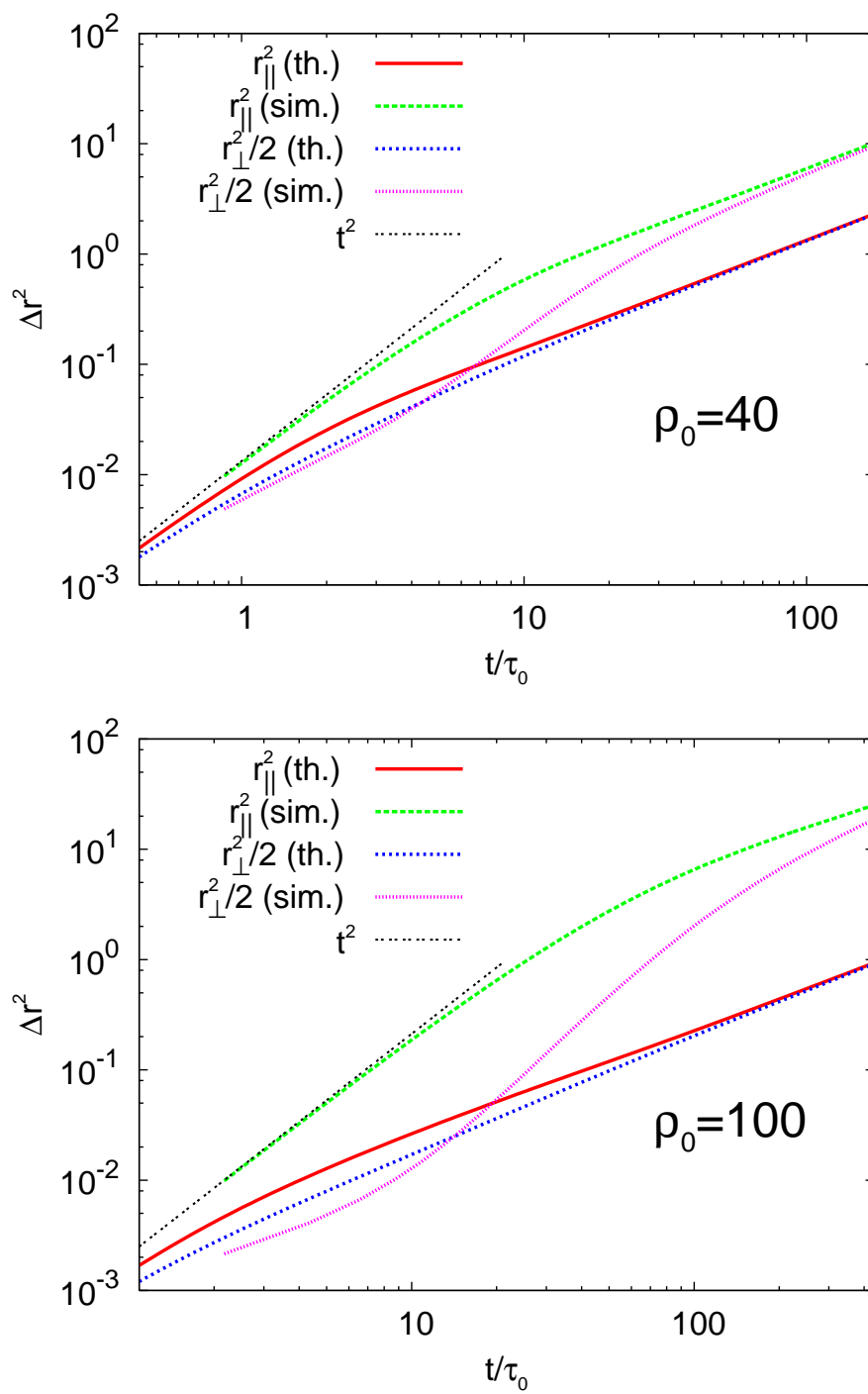


FIG. 5

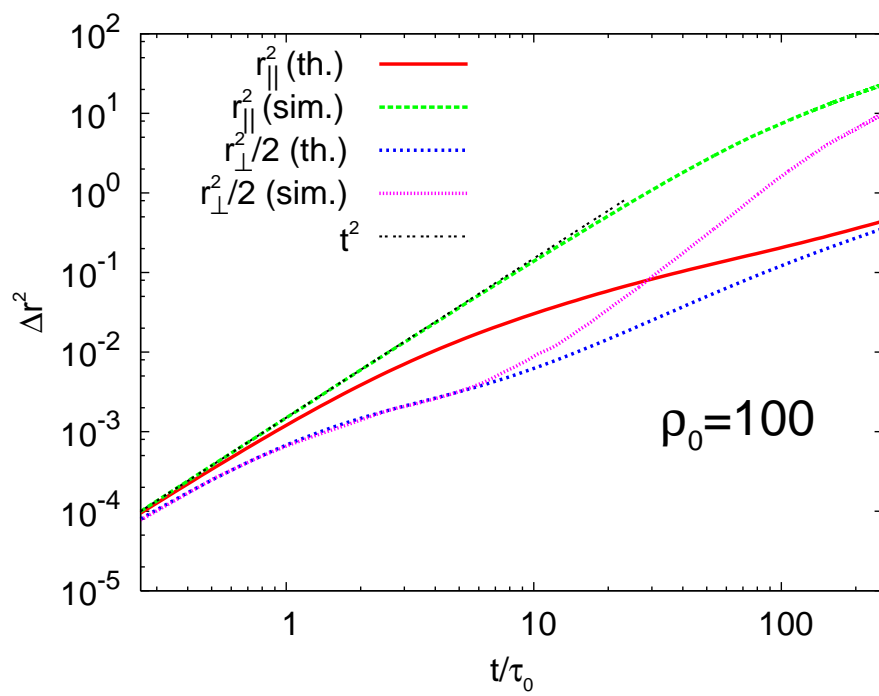


FIG. 6